จุฬาลงกรณ์มหาวิทยาลัย
ทุนวิจัย
กองทุนรัชดาภิเษกสมโภช

รายงานวิจัย

การพัฒนาระบบพลาสมาและโฟโตคะตาไลติก แบบหลายขั้นตอน สำหรับกำจัดมลสารทางอากาศ

โดย

สุเมธ ชวเดช

ตุลาคม ๒๕๔๖

ทุนวิจัย

กองทุนรัชดาภิเษกสมโภช

รายงานผลการวิจัย

การพัฒนาระบบพลาสมาและโฟโตคะตาไลติก แบบหลายขั้นตอน สำหรับกำจัดมลสารทางอากาศ

(Development of Multi-stage Plasma and Photocatalytic System for Removing Air Pollutants)

โดย

รองศาสตราจารย์ ดร. สุเมธ ชวเดช และคณะ

ตุลาคม 2546

ทุนวิจัย

กองทุนรัชดาภิเษกสมโภช

รายงานผลการวิจัย

การพัฒนาระบบพลาสมาและโฟโตคะตาไลติกแบบหลายขั้นตอน สำหรับกำจัดมลสารทางอากาศ

(Development of Multi-stage Plasma and Photocatalytic System for Removing Air Pollutants)

โดย

รองศาสตราจารย์ ดร. สุเมธ ชวเดช และคณะ

ตุลาคม 2546

ACKNOWLEDGEMENTS

The Ratchadapiseksompoch Fund, Chulalongkorn University is greatly acknowledged for financing this work. In addition, this research was also supported by The Petroleum and Petrochemical Technology Consortium in providing all analytical instruments. National Petrochemical (Public) Co., Ltd for donating ethylene is also appreciated. CPO Poon Arjpru who designed and fabricated the power supply unit is considerate to be an important contributor to the success of this project.

ชื่อโครงการวิจัย การพัฒนาระบบพลาสมาและโฟโตคะตาไลติกแบบหลายขั้นตอน สำหรับกำจัดมลสารทางอากาศ

ชื่อผู้วิจัย รองศาสตราจารย์ ดร. สุเมธ ชวเดช
ผู้ช่วยศาสตราจารย์ ดร. ปราโมช รังสรรค์วิจิตร
นางสาว กนกวรรณ ศักดิ์ตระกูล

เดือนและปีที่ทำวิจัยเสร็จ สิงหาคม 2546

บทคัดย่อ

มีเทคนิคอยู่หลายแบบที่ใช้ในการกำจัดมลสารอากาศ ได้แก่ การดูดซับ การกรองทางชีวภาพ และการเผาที่อุณหภูมิสูง อย่างไรก็ตามวิธีการเหล่านี้ จำเป็นที่จะต้องมีการบำบัดขั้นต่อไปและ/หรือต้องใช้พลังงานสูง ซึ่งทำให้ค่าใช้จ่ายในการบำบัดสูง การใช้พลาสมาและโฟโตคะตาไลติกเป็นทางเลือกหนึ่ง เนื่องจากทั้งสองเทคนิคสามารถดำเนินการที่สภาวะบรรยากาศ ซึ่งส่งผลให้ความต้องการพลังงานลดต่ำลง เมื่อเปรียบเทียบกับวิธีดั้งเดิมต่างๆ วัตถุประสงค์หลักในงานวิจัยนี้คือการพัฒนาระบบพลาสมาและโฟโตคะตาไลติกร่วมกันในการกำจัดมลสารระเหยง่าย เครื่องปฏิกรณ์พลาสมาแบบ 4 ขั้นตอนถูกสร้างขึ้นเพื่อทำการศึกษาการออกซิเดชั่นของก๊าซเอทิลีน ซึ่งถูกใช้เป็นตัวแทนมลสาร การเพิ่มค่าความต่างศักย์และจำนวนขั้นตอนของเครื่องปฏิกรณ์พลาสมาช่วยเพิ่มค่าการเปลี่ยนรูปของก๊าซเอทิลีน และการเลือกเกิดก๊าซคาร์บอนไดออกไซด์ ซึ่งแตกต่างกับผลกระทบที่เกิดจากการเพิ่มค่าความถี่และอัตราการไหลของสารตั้งต้น ไททาเนียมไดออกไซด์ทางการค้า (Degussa P25) ไททาเนียมไดออกไซด์โซล-เจล และ 1 เปอร์เซ็นต์แพลทินัมบนไททาเนียมไดออกไซด์โซล-เจล ถูกใช้เป็นโฟโตคะตาลีสท์ การใช้โฟโตคะตาลีสท์ทั้งหมดที่ศึกษา เพิ่มค่าการเปลี่ยนรูปของก๊าซเอทิลีนและก๊าซออกซิเจน พร้อมทั้งการเลือกเกิดคาร์บอนไดออกไซด์ตามลำดับดังนี้ 1 เปอร์เซ็นต์แพลทินัมบนไททาเนียมไดออกไซด์โซล-เจล>ไททาเนียมไดออกไซด์โซล-เจล>ไททาเนียมไดออกไซด์ทางการค้า (Degussa P25) ผลการเสริมของการทำงานร่วมกันของโฟโตคะตาลีสท์ในเครื่องปฏิกรณ์พลาสมา เป็นผลมาจากการกระตุ้นไททาเนียมไดออกไซด์ด้วยพลังงาน ซึ่งกำเนิดมาจากพลาสมา

Project title Development of Multi-stage Plasma and Photocatalytic System for Removing Air Pollutants

Name of the Investigators Assoc. Prof. Sumaeth Chavadej
Asst. Prof. Pramoch Rangsunvigit
Ms. Kanokwan Saktrakool

Year August 2003

ABSTRACT

A number of techniques for air pollutant removals are available such as adsorption, biofiltration and incineration. However, these techniques require further treatment and/or are energy-intensive leading to high treatment costs. Both plasma and photocatalysis are promising alternatives since these two techniques can be operated at ambient conditions resulting in low energy consumption as compared to the conventional methods. The main objective of this work was to develop a combined plasma and photocatalytic system for VOC removals. A four-stage plasma and photocatalytic reactor system was setup to study the oxidation of ethylene as a model pollutant. An increase in either applied voltage or stage number of plasma reactors enhanced C_2H_4 conversion and CO_2 selectivity which is in contrast with the effects of frequency and feed flow rate. The commercial TiO_2 (Degussa P25), sol-gel TiO_2, and 1%Pt/sol-gel TiO_2 were used as photocatalysts. The presence of all studied photocatalysts increased the C_2H_4 and O_2 conversions as well as CO_2 selectivity in the following order: 1%Pt/TiO_2 >TiO_2 >Degussa P25. The synergistic effect of photocatalysts presented in the plasma reactor is resulted from the activation of TiO_2 by the energy generated from the plasma.

รายนามคณะวิจัย

รศ.ดร. สุเมธ ชวเดช	หัวหน้าโครงการ
ผศ.ดร. ปราโมช รังสรรค์ค์วิจิตร	รองหัวหน้าโครงการ
น.ส. กนกวรรณ ศักดิ์ตระกูล	งานทดลอง
พ.จ.อ. พูน อาจปรุ	สร้างอุปกรณ์ทดลอง

TABLE OF CONTENTS

LIST OF TABLES

TABLE PAGE

LIST OF FIGURES

FIGURE **PAGE**

FIGURE **PAGE**

CHAPTER I
INTRODUCTION

Air pollutants affect both human health and environment. They can enter the human body by inhalation or touching. Their toxicity on human health can cause premature death, respiratory illness, alterations in the lung's defenses, and aggravation of existing cardiovascular disease. Furthermore, volatile organic compounds (VOC) are also precursors to smog, ozone and acidic precipitation (acid rain) and they can affect both terrestrial and aquatic ecosystems and finally global warming (Papaethimiou *et al.*, 1997). Emissions of pollutants come from many mobile sources and industrial processes including chemical industry and petroleum refineries.

There are various methods for air pollution abatement, such as liquid absorption, solid adsorption, scrubbing, precipitation, capture devices (fibers, membranes, condensers, etc.), biodegradation, thermal incineration, and catalytic combustion (Cheng, 1996). Combustion is the most effective way to achieve complete destruction of organic pollutants but the energy requirement for combustion is rather high. Non-thermal plasma and photocatalytic processes have been considered as promising alternatives to offer economical operation because the complete oxidation of organic pollutants at ambient temperature and pressure is possible. Moreover, main products from the plasma or photocatalytic processes are carbon dioxide, and water, which are environmental friendly. Plasma reactors have already been used to study different possible applications in control of toxic gases, volatile organic compounds, hazardous emissions, and for ozone synthesis (Eliasson *et al.*, 1987; Eliasson and Kogelschatz, 1991; Futamura *et al.*, 2001; and Huang *et al.*, 2001).

Non-thermal plasma is generated by applying electric field with high voltage across the metal electrodes to produce high-energy electrons that can decompose pollutants. Moreover, during plasma generation, light and active species including radicals, and ions are also produced apart from high-energy electrons. Previous work showed that the degradation of ethylene using a combined plasma and photocatalytic

process was greatly affected by the ethylene residence time (Harndumrongsak *et al.*, 2002).

In this work, a multi-stage plasma reactor unit with their own plasma generators was developed and tested for the ethylene oxidation. Moreover, the presence of TiO_2, used as a photocatalyst, was investigated the effect on ethylene oxidation reaction.

CHAPTER II
BACKGROUND AND LITERATURE SURVEY

2.1 Basic Principle of Plasmas

Gaseous plasma consists of negatively and positively charged particles in an otherwise neutral gas. The positively charged particles are mostly cations but the negatively charged particles can be either electrons and/or anions. The neutral species may be the mixture of free radical species with stable neutral gases. Plasma possesses two important properties (Eliasson and Kogieschatz, 1991).

1) Quasi-neutral property

The total density of negatively charged carriers must be equal to the total density of positively charged carriers.

2) Interaction with electromagnetic fields

Plasma can have some interactions upon the applying of an electromagnetic field due to the fact that they consist of charged particles.

Normally, plasma can occur in all states (Nasser, 1971). Plasma in solid is called solid-state plasma while plasma generated in liquid or gaseous states does not have any specific names. Only the gaseous plasma is shortly called as "plasma". There are many differences between plasma and gas. Their differences include pressure, distributions of charged-particle density in the entire plasma volume and temperature.

2.2 Generation of Plasmas

There are several means of generating charged particles to produce plasma, e.g., collisions between cosmic rays and gases in atmospheric layers. However, in the present study, an externally intense-electric field is applied across metal electrodes to cause the reduction in its "potential barrier" leading to the electrons leaving the electrode surface. The most interesting phenomena on the electrode surface under an extremely high-electric field is that many electrons can leak from the surface despite

its kinetic energy is too low to overcome the potential barriers. This phenomenon is known as "tunnel effect". Under a sufficiently high voltage, the plasma is first generated by the collisions between the electrons emitted from the surface of metal electrodes and the neutral molecules. This process of plasma generation is known as the "field" emission process (Eliasson and Kogelschatz, 1991).

The electrons liberated from the metal surface will immediately be accelerated to move corresponding to the direction of the electric field and then can collide with any neutral gaseous particles in their vicinity to form various ionized gases with excess free electrons. Accordingly, these free electrons can further move and collide with other species. As a result, a large quantity of electrons including the excited atoms and molecules, ions and radicals can be formed in the bulk of the gases within a very short period of time once the application of electric field is started. Several active species produced can further initiate various chemical reactions leading to the production of specific chemicals and the destruction of organic pollutants. Table 2.1 shows some important collision mechanisms of plasma chemistry (Eliasson and Kogelschatz, 1991).

Table 2.1 Collision mechanisms in the plasma (Nasser, 1971).

Collision	Reaction
Elastic Collision	$e^- + A \longrightarrow e^- + A$
Excitation	$e^- + A \longrightarrow e^- + A^*$
Ionization	$e^- + A \longrightarrow 2e^- + A^+$
Attachment	$e^- + A \longrightarrow A^-$
Dissociative Attachment	$e^- + B_2 \longrightarrow B^- + B$
Recombination	$e^- + B_2^+ \longrightarrow B_2$
Detachment	$e^- + B_2^- \longrightarrow 2e^- + B_2$
Ion Recombination	$A^- + B^+ \longrightarrow AB$
Charge Transfer	$A^\pm + B \longrightarrow A + B^\pm$
Electronic Decomposition	$e^- + AB \longrightarrow e^- + A + B$
Atomic Decomposition	$A^* + B_2 \longrightarrow AB + B$

The combined steps of the field emission process among these plasma species and the collisions between the species and the electrode surfaces are referred to as "electric discharges" phenomena (Nasser, 1971).

Plasma is divided into two types. The first type is "thermal plasma" or "equilibrium plasma". In this type, the temperature between gas and electron are approximately equal, which is close to thermodynamic equilibrium (Eliasson and Kogelschatz, 1991; and Grill, 1994). An essential condition for the formation of this plasma is sufficiently high working temperatures. An example of this plasma is arc discharge.

The second type is "non-thermal plasma" or "non-equilibrium plasma", which is characterized by low gas temperature and high electron temperature. Those typical energetic electrons may have energy ranged from 1 to 10 eV, which corresponds to the temperature of about 10,000 to 100,000 K (Rosacha *et al.*, 1993). This plasma can be classified into several types depending upon their generation mechanism, their pressure range and the electrode geometry (Eliasson *et al.*, 1987). Examples of this plasma are radio frequency discharge, microwave discharge, glow discharge, dielectric-barrier discharge, and corona discharge, which was used in this study.

The basically electrode geometry in corona discharge is a pair of wire and plate metal electrodes oriented in a perpendicular direction to each other. Corona discharge can solve the instability of the glow discharge at high pressure.

2.3 Basic Principle of Photocatalysis

Photocatalysis is a combination of photochemistry and catalysis implying that light and a catalyst usually a semiconductor are necessary to bring or accelerate a chemical transformation (Herrmann, 1999). When a semiconductor is irradiated with light at an appropriate wavelength, most often in the ultraviolet spectral range, it generates oxidant species, which can convert most organic materials into CO_2, water and inorganic compounds. A semiconductor such as TiO_2 is specified by the electronic band structures, which are occupied valance band (vb) and unoccupied conductance band (cb). When a semiconductor absorbs light, the light energy can force the electrons at the occupied valance band to move to the unoccupied

conductance band that has a higher energy level, and consequently the positive holes (h^+) are formed. The difference of both energy levels is called energy band gab. If gases are localized by trapping at both energy bands long enough, both reduction and oxidation reactions will occur as shown in Figure 2.1.

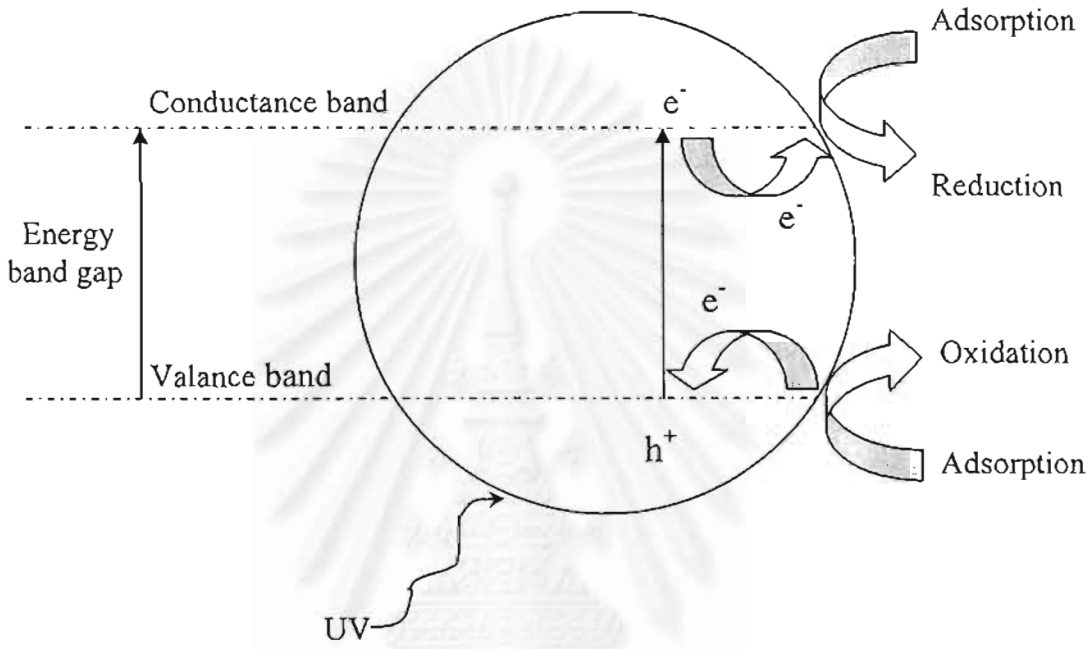

Figure 2.1 The mechanism of photocatalytic process of a semiconductor (Litter, 1999).

There are possible reactions that can occur when a semiconductor absorbs a photon (hν) of a suitable wavelength (Robertson, 1996).

Light absorption	$SC + h\nu$	$\longrightarrow$	$e^- + h^+$	(2.1)
Recombination	$e^- + h^+$	$\longrightarrow$	Heat/light	(2.2)
Oxidation	$D + h^+$	$\longrightarrow$	D^+	(2.3)
Reduction	$A + e^-$	$\longrightarrow$	A^-	(2.4)

The electron-hole pairs can recombine either directly or indirectly by radiative and nonradiative processes in a few nanoseconds. The problem of photocatalysis is a recombination reaction between the electrons and the positive holes because it

inhibits the redox reactions. To solve this problem, electron scavengers such as oxygen molecules are added since it can trap electrons out from the positive hole to form superoxide radical ion (O_2^{*-}) leading to the sequential formation of hydroxyl radical (Litter, 1999), which is essential species in the photocatalytic process since the hydroxyl radical is the most powerful oxidant.

$$O_2 + e^- \longrightarrow O_2^{*-} \quad (2.5)$$

$$2H_2O + O_2^{*-} \longrightarrow 2H_2O_2 \quad (2.6)$$

$$H_2O_2 \longrightarrow 2OH^* \quad (2.7)$$

Water is a major source of hydroxyl group as the primary oxidant, which is generated by dissociative adsorption. Hence, in the absence of water vapor, the photocatalytic oxidation of organic is seriously retarded and total mineralization to CO_2 does not occur. Since hydroxyl radical has a high oxidation potential, it can react rapidly and non-selectively with most organic compounds into carbon dioxide, water and other inorganic compounds (De Lasa *et al.*, 1992). Possible reaction mechanisms involving hydroxyl ions as photo hole traps are summarized below (Peral *et al.*, 1997).

$$TiO_2 + h\nu \longleftrightarrow h^+ + e^- \longleftrightarrow h^+ - e^- \quad (2.8)$$

$$HO^- + h^+ \longrightarrow HO^* \quad (2.9)$$

$$O_{2ads} + e^- \longrightarrow O_2^-{}_{ads} \quad (2.10)$$

$$HO^* + O_2^-{}_{ads} \longrightarrow HO_2^* + O^-_{ads} \quad (2.11)$$

$$HO_2^* + e^- \longrightarrow HO_2^- + O^-_{ads} \quad (2.12)$$

$$HO_2^- + h^+ \longrightarrow HO_2^* \text{ (hole-trap)} \quad (2.13)$$

2.4 Types of Semiconductors

A semiconductor used as photocatalyst should be either oxide or sulfide of metals, such as TiO_2, CdS, and ZnO. The energy band gap of the semiconductor must be matched with the energy gained from a light source. TiO_2 is a popular one since the band gap is around 3.1 eV, which can be simply activated in the near

ultraviolet light (~380 nm). Other advantages of TiO_2 include more stable and insoluble in aqueous solution, high reactive catalyst, nontoxic and inexpensive catalyst. Furthermore, TiO_2 is corrosion resistant and does not lose activity when reused (De Lasa *et al.*, 1992).

TiO_2 is classified into three different phases, which are anatase, rutile and brookite. In the anatase phase, it has been observed that it is more active and stable than the other two phases because of its higher surface area. Rutile is a thermally stable form at high temperatures, whereas heating amorphous TiO_2 produces brookite.

Other types of semiconductors such as ZnO or CdS may not be applicable due to their toxicity. Table 2 compiles the common properties of several semiconductors.

Table 2.2 Band positions of some common semiconductor used as photocatalysts (Robertson, 1996).

Semiconductor	Valence band (eV)	Conductance band (eV)	Band gap (eV)	Band gap Wavelength (nm)
TiO_2	+3.1	+0.1	3.1	380
SnO_2	+4.1	+0.3	3.9	318
ZnO	+3.0	-0.2	3.2	390
ZnS	+1.4	-2.3	3.7	336
WO_3	+3.0	+0.2	2.8	443
CdS	+2.1	-0.4	2.5	497
CdSe	+1.6	-0.1	1.7	730
GaAs	+1.0	-0.4	1.4	887
GaP	+1.3	-1.0	2.3	540

2.5 Related Research Works

2.5.1 Plasma

Futamura and Yamamoto (1997) studied the effects of oxygen and moisture on trichloroethylene (TCE) decomposition by using a pulsed corona reactor. When nitrogen gas was used as a carrier gas in the dry condition, higher decomposition efficiency of TCE was obtained. They suggested that active oxygen species in air were not responsible for the initial processes of halogenated olefin because oxygen competed with TCE in the process of electron transfer. Negative effect of moisture on TCE decomposition efficiency indicates quenching of high-energy electrons and excited nitrogen and oxygen molecules as an energy transfer agent. Under aerated conditions, triplet oxygen molecules scavenged intermediate carbon radicals derived from the TCE decomposition to finally give CO and CO_2, resulting in much lower by-product yields below their threshold limit values than that under deaerated conditions.

Futamura *et al.* (1999) investigated plasma chemical behavior of hazardous air pollutants (HAP's) ($Cl_2C{=}CCl_2$, $Cl_2C{=}CHCl$, $Cl_3C\text{-}CH_3$, $Cl_2CH\text{-}CH_2Cl$, CH_3Cl, CH_3Br, and benzene) by using a ferroelectric packed-bed plasma reactor. It was found that oxidation of CO to CO_2 was a slow reaction in plasma, and the formation of CO or CO_2 was mainly resulted from different precursors. An increasing oxygen content did not improve CO_2 yield because of the slow backward reaction of CO_2 to CO in air.

Sano *et al.* (1997) studied the removal of acetaldehyde and skatole by a corona-discharge reactor. They found that under the pure nitrogen atmosphere, methane was produced as a reaction by-product from the removal of acetaldehyde but no reaction by-product was produced from the removal of skatole. It was explained that skatole was removed on the basis of its electron attachment. When oxygen was added, the removal efficiencies of acetaldehyde and skatole increased greatly since ozone (O_3) was produced inside the reactor. It was estimated that the O_3 produced contributed half of the removal efficiency of acetaldehyde. For the mixture of acetaldehyde and skatole under the mixed gas of N_2 and O_2, it was found that the

coexisting skatole inhibited the formation of the negative ion clusters of acetaldehyde.

CO_2/CH_4 reformed by glow discharge plasma with and without micro-arc formation using a Y-type reactor was studied by Huange *et al.* (2000). It was reported that the system with the formation of micro-arcs produced more CO as well as higher energy efficiencies than that without the micro-arc formation. Furthermore, with an increase in the CO_2 to CH_4 ratio, the CO selectivity increased, and less coke formed.

Malik and Malik (1999) investigated a combined system of cold plasma and a catalyst for VOC destruction. They found that the addition of a suitable catalyst particularly a supported noble metal catalysts such as platinum, palladium, rhodium and ruthenium, could activate CH_4 at relatively low temperatures with faster rates and could further improve the efficiency as well as the selectivity of the desired products. The use of noble metal electrodes was found to enhance the conversion of CH_4 to C_2 hydrocarbons in a pulsed corona discharge with the following order: Platinum > Palladium > Copper.

Thanyachotpaiboon *et al.* (1998) studied the conversion of CH_4 to higher hydrocarbons in AC non-equilibrium plasma. It was shown that CH_4 conversion initially increased with increasing voltage and residence time above the breakdown voltage because a higher density of the electrons gives a higher probability of a CH_4 molecule interacting with electrons to form active species. CH_4 conversion also increased when He and C_2H_6 were added in the feed stream. He and C_2H_6 both appeared to be more easily activated than CH_4 and so the presence of He or C_2H_6 enhance CH_4 conversion.

Tsai *et al.* (2001) studied the product distribution of methanethiol (CH_3SH) decomposition in a RF plasma reactor. In the absence of oxygen, over 83.7 % of the total sulfur input was converted to carbon disulfide (CS_2) at 60 W. When oxygen was added, the main product of sulfur was shifted to SO_2 due to the thermodynamic stability. Oxygen was believed to play an important role for inhibiting dihydrogen sulfide (H_2S), dimethyl sulfide (DMS), and dimethyl disulfide (DMDS) formation. The mole fractions of methane, ethylene, and acetylene were rapidly decreased as the O_2/CH_3SH ratio increased from 0 to 3, and did not change when the O_2/CH_3SH ratio

was further increased to 4.5. At a higher O_2/CH_3SH ratio and increasing input power, CO could be converted to CO_2 by reacting with O, OH, O_2, HCO, and H_2O. The mechanism of the formation and decomposition of CO and CO_2 are shown below.

CO formation and decomposition

$$CH + (O, O_2) \longleftrightarrow CO + (H, OH) \quad (2.14)$$

$$CH_2 + (O, O_2) \longleftrightarrow CO + (2H \text{ or } H_2, H_2O, OH+H) \quad (2.15)$$

$$HCO + (M, O, O_2, H, OH) \longleftrightarrow CO + (H_2, H+M, H_2O, HO_2, OH) \quad (2.16)$$

$$CS + (O, O_2) \longleftrightarrow CO + (S, SO) \quad (2.17)$$

CO_2 formation

$$CO + (M, O, O_2, HO_2, OH) \longleftrightarrow CO_2 + (M, O, H, OH) \quad (2.18)$$

$$HCO + (CO, O) \longleftrightarrow CO_2 + (CH, H) \quad (2.19)$$

$$CH_2 + O_2 \longleftrightarrow CO2 + (2H \text{ or } H_2) \quad (2.20)$$

Kruapong (2000) determined the effects of voltage, frequency, and flow rate on CH_4 conversion in corona discharge. Higher voltage, lower frequency, and lower flow rate of CH_4 gave higher conversion of CH_4 and O_2 and higher selectivity to CO_2, and H_2.

Suttiruangwong (1999) performed experiments with and without catalysts and found that the non-catalytic system gave much higher CH_4 conversion than the catalytic system and products mainly consisted of C_2 hydrocarbons.

Although the nonthermal plasma technology shows high performance for the removal of VOCs, a major disadvantage of this technique is the formation of some unexpected toxic products such as NOx, phosgene, etc.

2.5.2 Photocatalysis

Einaga *et al.* (2001) examined benzene conversion by using platinized titania. Without Pt, benzene was converted into CO and CO_2 but CO could not be further oxidized to CO_2. On the other hand, as the amount of Pt loaded on TiO_2 was increased, the rate of the CO photooxidation was increased while the rate of benzene removal was almost unchanged. Moreover, it was found that complete oxidation of

benzene to CO_2 could be achieved by using the hybrid catalysts comprising pure TiO_2 and platinized TiO_2.

Obuchi *et al.* (1999) studied the photocatalytic decomposition of acetaldehyde over TiO_2/SiO_2 and Pt-TiO_2/SiO_2. They found that the unplatinized catalyst gave a conversion of acetaldehyde and a yield of CO_2 about 10 % less than the platinum loaded one. That is because platinum may help increasing the adsorption of the reactant, which was confirmed by calculation based on Langmuir-Hinshelwood. Platinum does not only increase the rate of the reaction, but also lower temperature required for the catalyst regeneration. Moreover, the FT-IR results showed the band of carbonic acid, suggesting the existence of acetic acid and/or formic acid as an intermediate adsorbed on the catalyst.

Nakamura *et al.* (2000) studied the photocatalytic activity of plasma-treated TiO_2 and raw TiO_2 powder for eliminating NO. They reported that the NO removal by both photocatalysts increased with decreasing wavelength. In the case of plasma-treated TiO_2 catalyst, the reaction occurred above 450 nm due to the change in the electronic state of TiO_2 caused by the reduction. The oxygen vacancies are formed in the crystal lattice of TiO_2 by the plasma treatment, maintaining the anatase structure. Furthermore, it was explained that the oxygen vacancy state between the valence and conductance bands are newly formed and then react with O_2 or O-species to produce reactive oxygen species such as O^- and atomic oxygen

Zhang *et al.* (2001) investigated the effect of TiO_2 on the decomposition of NO. The rate of NO conversion decreased with a decrease in the intensity of the incident UV light. Moreover, it was found that the reaction efficiency was high at the beginning of the reaction, and then gradually decreased with the reaction time.

CHAPTER III
MATERIALS AND METHODS

3.1 Materials

3.1.1 Catalyst Preparation Materials

Titanium dioxide (100% purity) was obtained from J.J. Degussa Hüls (T) Co. Ltd. Platinum (II) 2, 4-pentanedionate, Pt $(C_5H_7O_2)_2$ (49.8%Pt) was obtained from Alfa Aesar. Tetraethylorthotitanate (TEOT) (100% purity) was supplied by Fluka. Ethanol with 99.7% purity was supplied by BDH. Nitric acid (65%) was supplied by Lab-Scan. All chemicals were used as received. Distilled water was used throughout this study.

3.1.2 Reactant Gases

Helium (He) with 99.95% purity and Oxygen (O_2) with 99.5% purity were obtained from Thai Industrial Gas (Public) Co., Ltd. Ethylene (C_2H_4) with 99.99% purity was obtained from National Petrochemical (Public) Co., Ltd.

3.2 Catalyst Preparation

Catalysts used in this work were prepared by dipping a glass ring or glass wool as the catalyst support in a slurry of a commercial TiO_2 (Degussa P25) or sol-gel TiO_2. The glass ring was 7 mm OD, 5 mm ID, and 10 mm long. The surface of the glass ring was etched by HF before coated with the catalyst. The glass wool was pretreated to remove all undesirable matters such as wax and binder at 450°C for 2.5 h. The treated glass wool was then cut to the size of 3x3 cm^2.

To prepare Degussa P25 coated on a glass ring or glass wool, Degussa P25 slurry was prepared by mixing 0.6 g of Degussa P25 with 29.4 ml of distilled water. The glass ring or glass wool was then immersed in this slurry for 5 min and dried in an oven at 100 °C for 15 min. The procedure was repeated 8 times for the glass ring and one time for the glass wool. The coated glass ring or glass wool was annealed in

a furnace at 300°C for 3 h, and cooled to room temperature with a cooling rate of 50 °C/min. The catalyst was white after annealing. The amount of TiO_2 loading was about 0.003 g on the glass ring and 0.008 g on the glass wool.

For a glass ring or glass wool coated with sol-gel TiO_2, TiO_2 slurry was prepared by mixing 1.5 g of Titanium (IV) ethoxide (TEOT) with 20 ml of ethanol and 6 drops of nitric acid. The coating procedure was the same as previously described except using only 400°C and 5 h instead of 300°C and 3 h for annealing.

To prepare 1% Pt/TiO_2, 0.005 g of $Pt(C_5H_7O_2)_2$ and 2.83 g of TEOT were dissolved in 38.07 ml of ethanol and 14 drops of nitric acid. The same procedures of coating and calcination were carried out as described above.

3.3 Catalyst Characterization

Surface areas of the prepared catalysts were determined by a surface area analyzer(Quantachrom,Autosorb-1). The samples were degassed at 200 °C overnight before the analysis. Nitrogen was used as a probe gas. A catalyst sample was dried and outgassed in the sample cell at 200 °C for at least 4 h before adsorption. The specific area of each catalyst was calculated from the 5 points adsorption isotherm. The results were analyzed by the Autosorb ANAGAS software version 2.10.

Crystalline phases of the catalysts were determined by an X-ray diffractometer (Rigaku, RINT-2200) equipped with a graphite monochromator and a Cu tube for generating CuK_α radiation (λ = 1.5406 ^{0}A) at a generator voltage of 40 kV and a generator current of 30 mA. A nickel filter was used as the K_α filter. The goniometer parameters were divergence slit = 1°(2θ); scattering slit = 1°(2θ); and receiving slit = 0.3 mm. The catalyst sample was held on a glass slide holder and was examined between 5 to 90°(2θ) range at a scanning speed of 5°(2θ)/minute and a scan step of 0.02°(2θ). The digital output of proportional X-ray diffractor and the goniometer angle measurements were sent to an online microcomputer to record the data and subsequent analysis. The X-ray patterns of the catalysts were compared with that of Degussa P-25.

3.4 Oxidation Reaction Experiment

Schematic diagrams of the experimental set-up and the power supply in this work are shown in Figure 3.1 and 3.2, respectively. Reactant gases, ethylene, oxygen, and helium, controlled by mass flow controllers, were introduced into the first reactor at room temperature and atmospheric pressure. Before the reactant

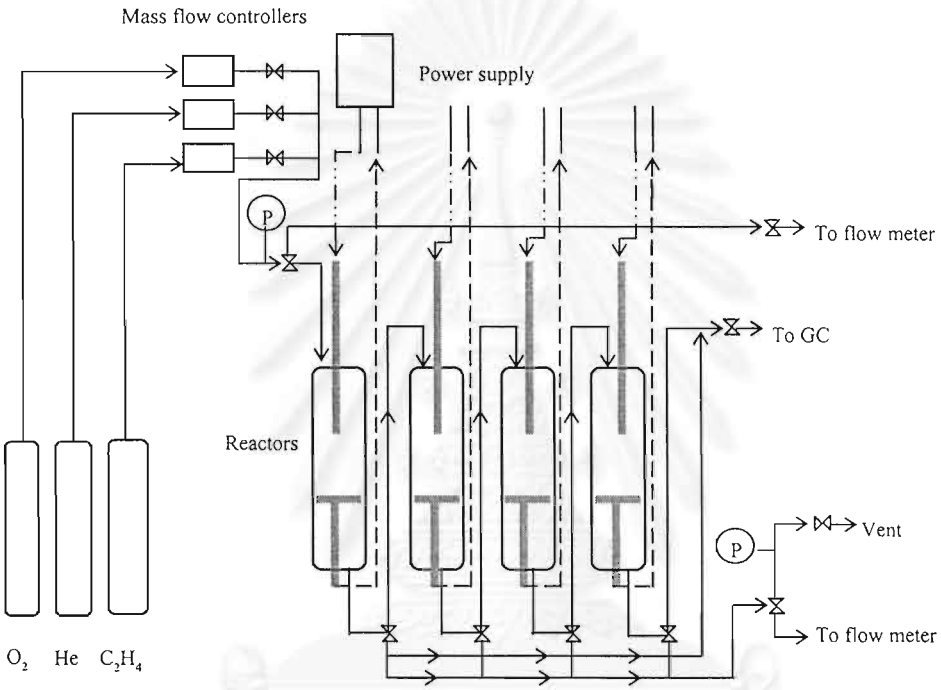

Figure 3.1 Schematic diagram of the experimental set-up

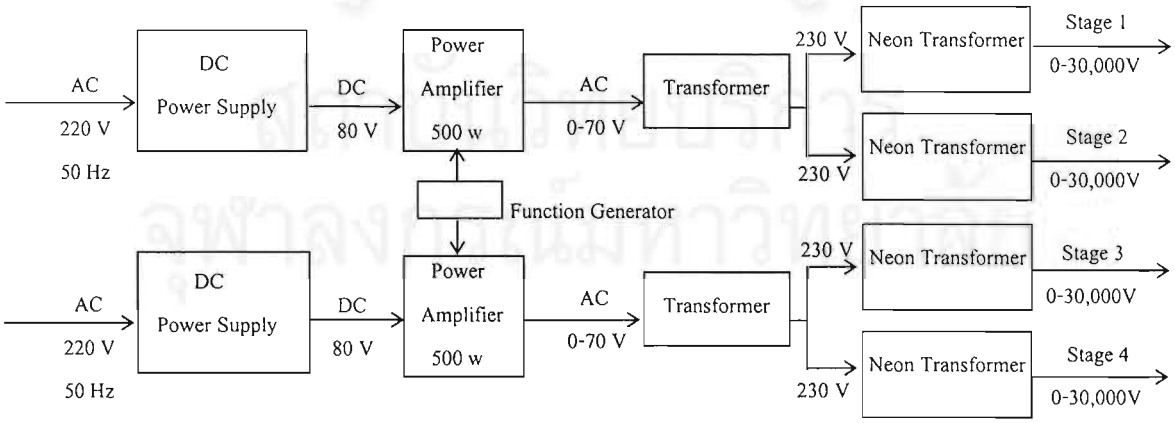

Figure 3.2 Schematic diagram of the power supply

gases passed through the mass flow controllers, any foreign particles in the feed gases were trapped by 0.7 μm in-line filters. The feed mixture was controlled to have 3% ethylene and 15% oxygen with helium balance. Helium was used instead of air since it is easy to control the composition of feed gas. The four reactors which were made of quartz tubes with 10 mm OD and 8 mm ID were arranged in a series. Plasma was generated in each reactor via a pair of stainless steel pin and plate electrodes. The pin and plate electrodes were located at the center of each reactor. The power used to generate plasma was alternative current power, 220V and 50 Hz, which was transmitted to a high voltage current. The output voltage was increased up to 130 times and the signal of the alternative current was a sine form. The glass ring or glass wool coated with either the sol-gel TiO_2 or Degussa P25 was packed in the space between the two electrodes as shown in Figure 3.3.

The experiment was started with the feed gas composition analysis by a gas chromatograph (Perkin-Elmer, AutoSystem GC) equipped with a thermal conductivity detector. The GC conditions used were summarized as follows:

Injection temperature:	160 °C
Oven temperature:	120 °C for 5 min
	170 °C (heating rate 10 °C /min)
	for 20 min
Carrier gas:	High purity helium
Carrier gas flow rate:	30 mL/min
Column type:	Packed column (Carboxen 1000)
Detector temperature:	200 °C

A ratio of oxygen to ethylene was set constant at 5:1. After the concentration of the feed mixture was constant, the supply power unit was turned on. After 30 min, the composition of the effluent was analyzed every 30 min until the outlet gas composition was constant. Effects of the stage number of the plasma and photocatalytic system on the ethylene removal and product selectivities were investigated by turning off one by one reactor with the fourth one first. The calculation of product selectivities is based on the carbon content of the converted ethylene fraction.

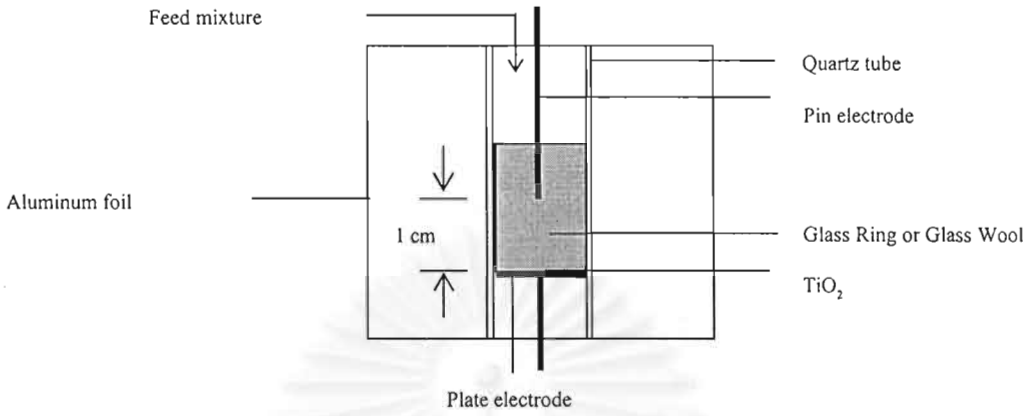

Figure 3.3 Schematic diagram of each reactor.

3.5 Studied Conditions

The experiments were divided into 2 main parts: with and without photocatalyst. All parameters studied were summarized in Table 3.1. All experiments were conducted under ambient conditions.

Table 3.1 Experimental conditions

Effects	Number of plasma generator(s)	Gas flow rate (mL/min)	AC frequency (Hz)	% TiO_2 loading(g)
Plasma	1-4	40-240	50-800	-
Plasma and Photocatalyst	1-4	160	50-200	0.008

In this study, a residence time of each rector is defined by the reaction volume between the two electrons divided a feed gas flow rate. A residence time of the system is calculated from a summation of the residence time of each reactor.

CHAPTER IV
RESULTS AND DISCUSSION

4.1 Catalyst Characterization

BET surface areas of commercial TiO_2 (Degussa P25), sol-gel TiO_2, and 1%Pt/ sol-gel TiO_2 were 63.77, 103.1, and 103.5 m^2/g, respectively. The crystal structures of the studied photocatalysts identified by XRD patterns are shown comparatively in Figure 4.1. The commercial TiO_2 (Degussa P25), sol-gel TiO_2, and 1%Pt/ sol-gel TiO_2 show the anatase peaks observed prominently at the same position of 2θ whereas no peaks of platinum at $2\theta = 40^{\circ}$ and 48° were observed. It suggests that Pt can be dispersed well on TiO_2. From the XRD results, it indicates that the commercial TiO_2 is more crystalline than both sol-gel TiO_2 catalysts since the sol-gel TiO_2 was calcined at a relative high temperature of 400°C. Moreover, the surface morphology of the studied catalysts coated on glass wool was also examined by using a scanning electron microscope (SEM). Figure 4.2 shows the topography of Degussa P25, sol-gel TiO_2, and 1% Pt/ sol-gel TiO_2. According to the figure, the surface characteristics of sol-gel TiO_2 and 1%Pt/ sol-gel TiO_2 prepared by the sol-gel method are smoother than Degussa P25.

4.2 Effects of Frequency

4.2.1 Effects on Ethylene and Oxygen Conversions

Figures 4.3 and 4.4 show the effects of frequency on C_2H_4 and O_2 conversions, respectively. The conversions of C_2H_4 and O_2 decreased with increasing frequency in the range of 50 to 700 Hz. The explanation is that a higher frequency results in lower current that corresponds to the reduction of the number of electrons generated (Morinaga and Suzuki, 1961 and 1962) as confirmed in Figure 4.5. Consequently, the opportunity of collision between electrons and O_2 molecules decreases. At each frequency, the conversions of C_2H_4 and O_2 increased as an increase in the stage number of reactors. This is because the residence time is increased with increasing the stage number.

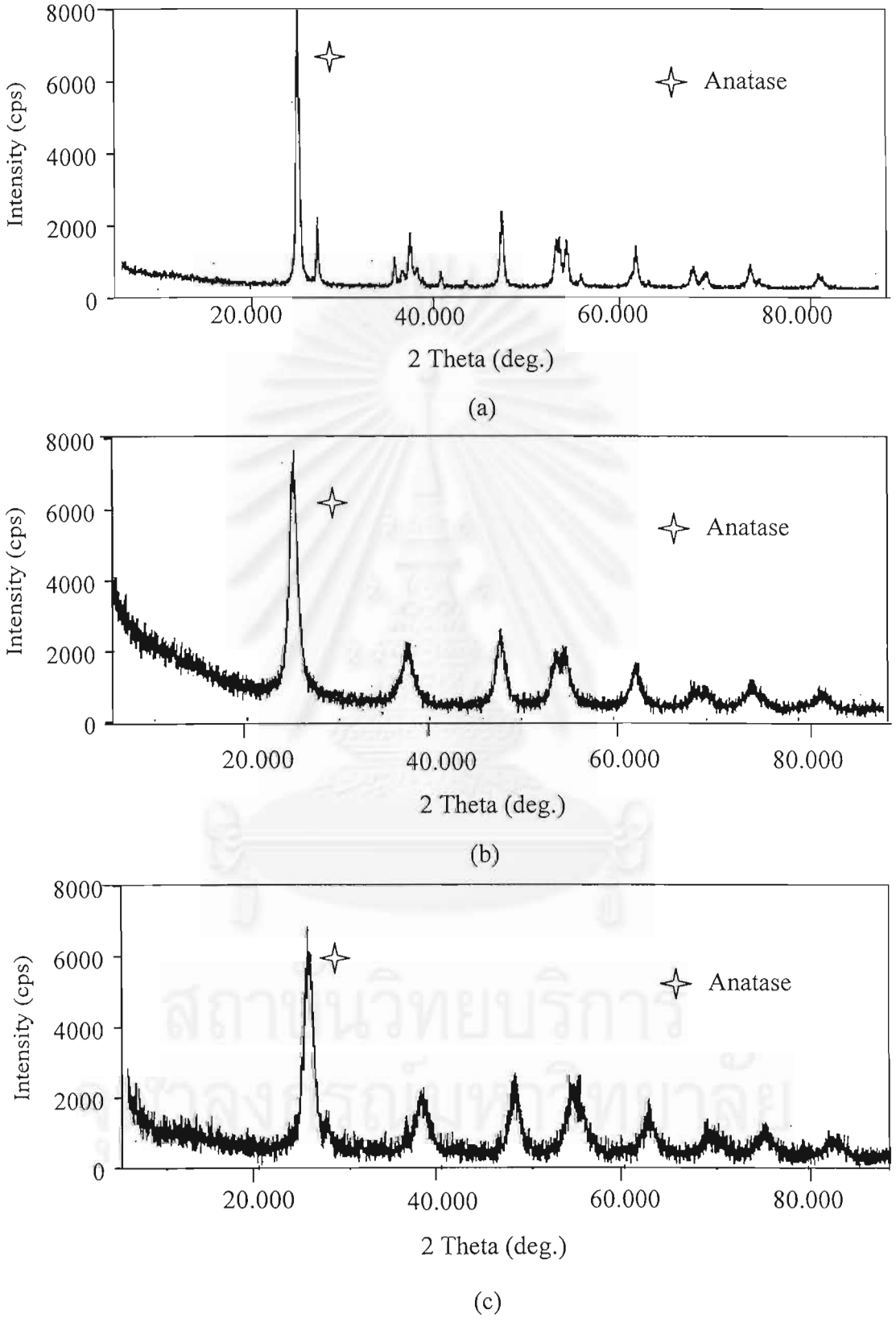

Figure 4.1 XRD patterns of (a) Degussa P25, (b) sol-gel TiO_2, (c) 1%Pt/ sol-gel TiO_2.

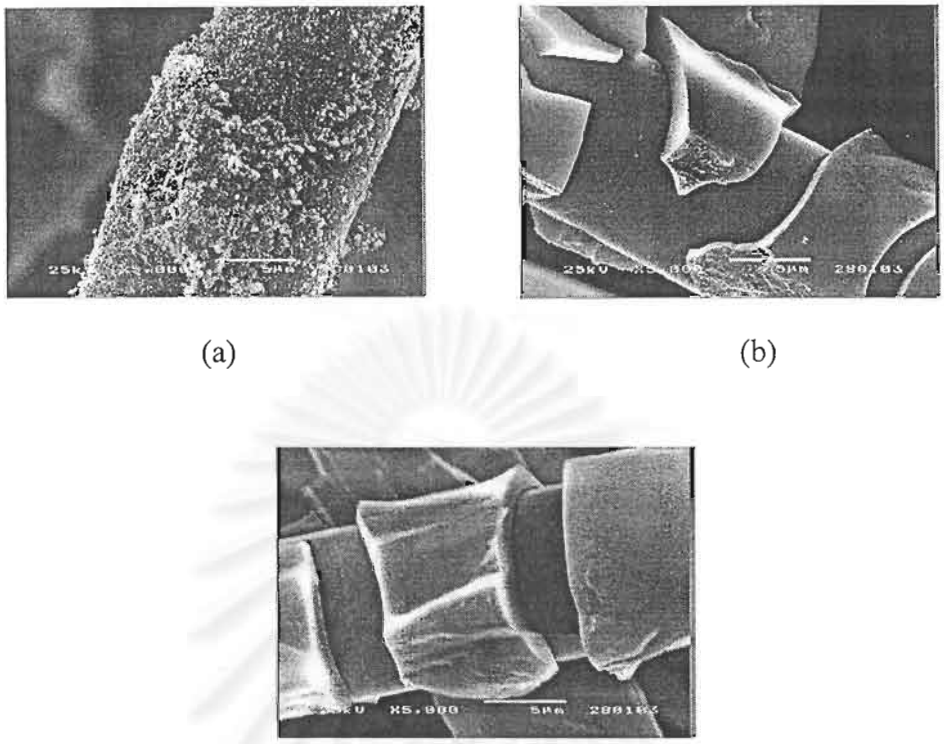

(a) (b)

(c)

Figure 4.2 SEM micrographs of (a) Degussa P25, (b) sol-gel TiO_2, (c) 1%Pt/sol-gel TiO_2 coated on glass wool sheet.

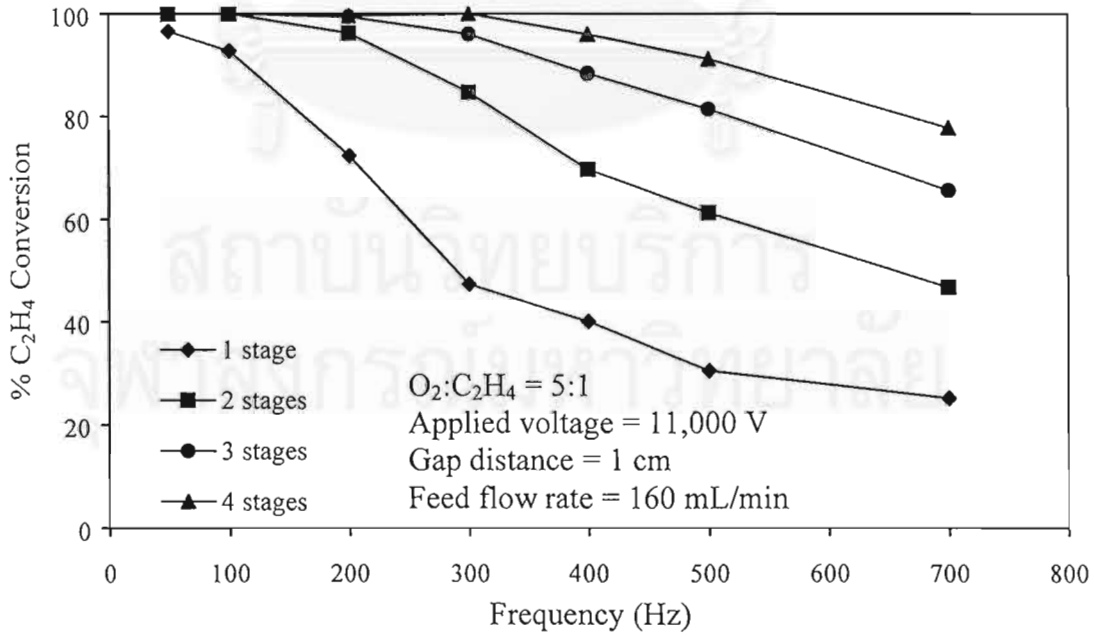

Figure 4.3 Effect of frequency on C_2H_4 conversion at different stage number of reactors.

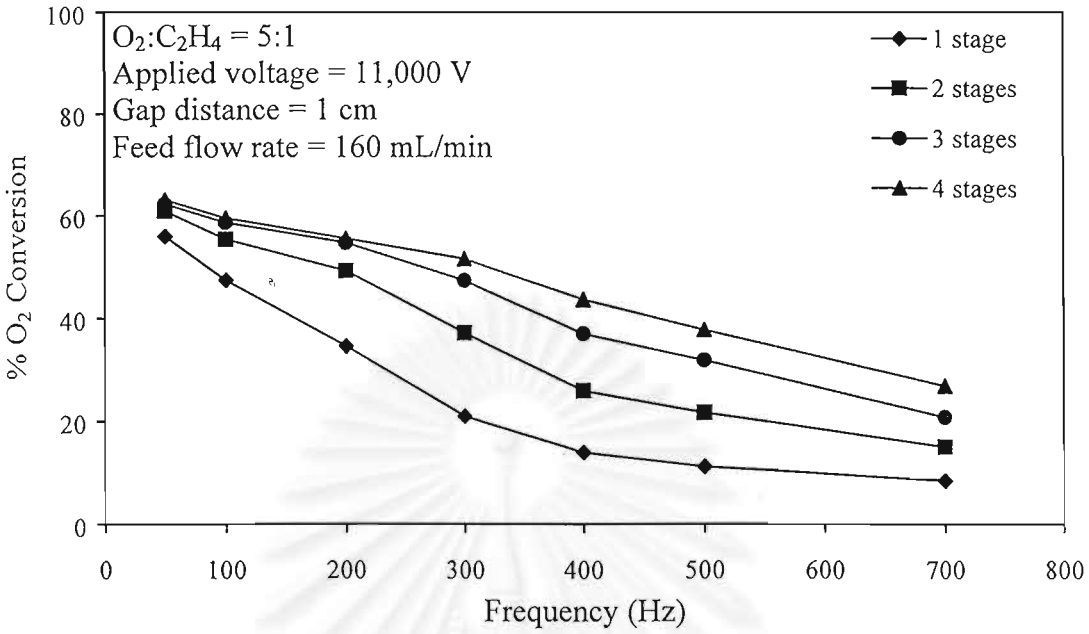

Figure 4.4 Effect of frequency on O_2 conversion at different stage number of reactors.

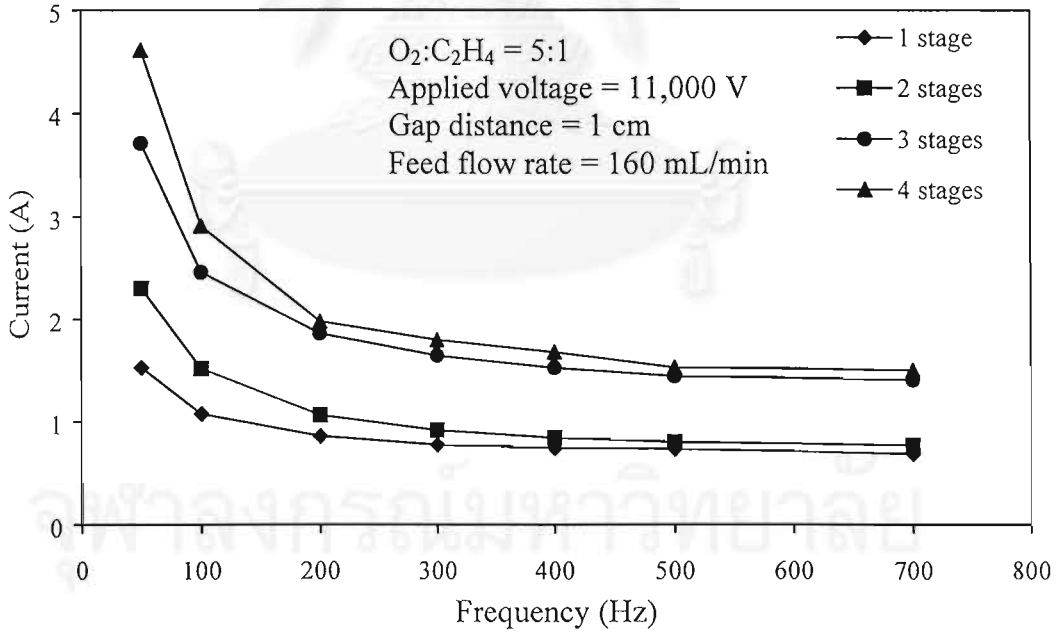

Figure 4.5 Effect of frequency on current at different stage number of reactors.

4.2.2 Effects on Product Selectivities

The effects of applied frequency on CO and CO_2 selectivities are shown in Figures 4.6 and 4.7, respectively. When the frequency increased, the CO_2 selectivity decreased whereas the CO selectivity increased. As mentioned before, at a lower frequency, there is a larger number of electrons generated from the electrodes as it shown in Figure 4.5. These electrons and O active species are accelerated to have higher energy resulted from higher electric field strength. Consequently, the reaction between the O active species and CO becomes more effective leading to a higher CO_2 selectivity. For any given frequency, the CO_2 selectivity also increased while CO selectivity decreased with increasing stage number of plasma reactors because the electrons have more chances to break down O_2 to produce the oxygen active species.

As AC discharge is applied, each electrode performs alternatively as an anode and cathode. The space charge between the two electrodes is eliminated and then a new space charge is initiated every half cycle. With increasing frequency, a faster reversal of the electric field reduces the decay of the space charge. Acceleration of

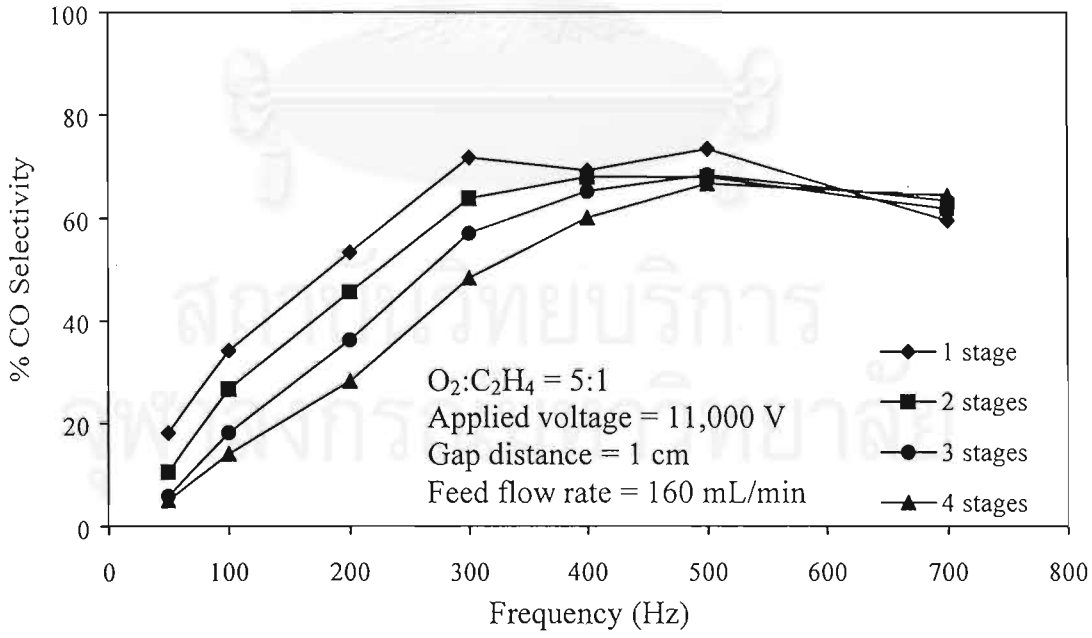

Figure 4.6 Effect of frequency on CO selectivity at different stage number of reactors.

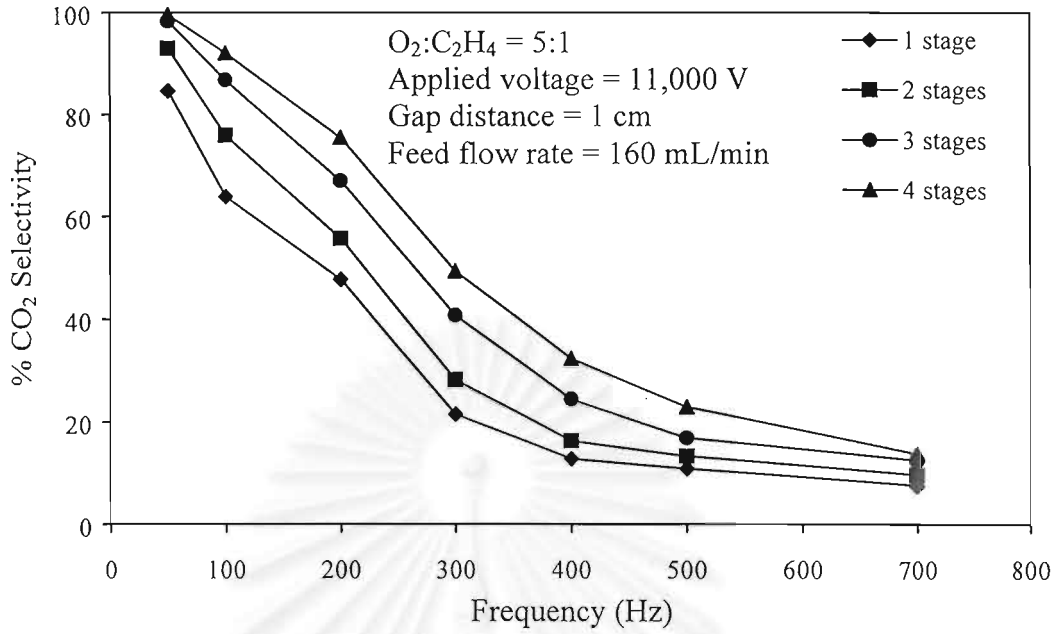

Figure 4.7 Effect of frequency on CO_2 selectivity at different stage number of reactors.

the remaining space charge by the reversing electric field can decrease the amount of current needed to sustain the discharge (Hill, 1997). Moreover, the alternating behavior has been proven effectively in eliminating contaminant accumulation on the electrodes resulting in increasing conversions as compared to DC discharge (Liu *et al.*, 1996). The effect of frequency on the conversions and selectivities is from the space charge (electrons and ions) characteristics of the discharge, even though the power is constant.

The effect of frequency on power consumption to break down each C_2H_4 molecule is shown in Figure 4.8. As can be seen from Figure 4.8, the optimum power is obtained with the frequency in the range of 200 – 500 Hz. Since a lower frequency results in a larger number of electrons generated leading to higher power consumption. On the other hand, a higher frequency corresponds to reduce electrons generated form electrodes leading to reducing C_2H_4 decomposition. To obtain the minimum power consumption as well as to have a relatively high C_2H_4 conversion, 200 Hz was selected for next experiments. In addition, the amounts of by-products at 200 Hz are lower than at higher frequencies as shown in Table 4.1.

Interestingly, other hydrocarbon products were found very low in the studied range of frequency except large amounts of hydrocarbons were produced at high frequency (greater than 400 Hz). It can be concluded that under the optimum frequency of 200 Hz, CO and CO_2 are mainly end products of the system. From the viewpoint of air pollution control, it is reasonable to discuss comprehensively our experiment results on selectivities of CO and CO_2.

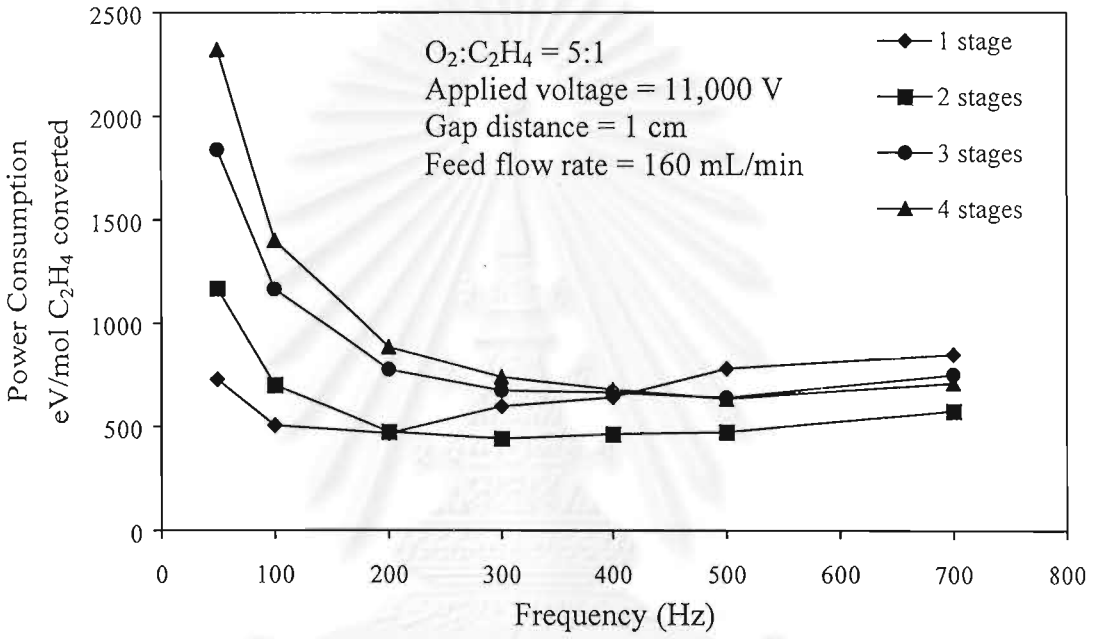

Figure 4.8 Effect of frequency on power consumption of C_2H_4 at different stage number of reactors.

4.3 Effects of Applied Voltage

As be known, it is not possible to measure the voltage across the electrodes of the reactor (high side voltage) because of its non-equilibrium in nature. The low side voltage was measured instead and then the high side voltage was calculated by multiplying with a factor of 130.

4.3.1 Effects on Ethylene and Oxygen Conversions

Figures 4.9 and 4.10 show the effects of applied voltage on C_2H_4 and O_2 conversions, respectively. The conversions of C_2H_4 and O_2 increased slightly with

increasing applied voltage in the range of 9,000 to 15,000 V, which is in contrast with the effect of frequency. The explanation is that a higher voltage results in higher

Table 4.1 Effect of frequency on by-product selectivities at a feed flow rate of 160 ml/min, 11,000 V, and a gap distance of 1 cm with different stage number of reactors

Types of by-products	% Selectivities						
	Frequency, Hz						
	50	100	200	300	400	500	700
1 Stage							
H_2	U	U	U	U	U	12.52	15.53
CH_4	0.16	U	U	0.27	1.24	1.54	2.45
C_2H_2	0.13	U	0.26	U	0.16	0.47	0.16
C_2H_6	0.06	U	U	U	U	1.01	0.15
2 Stages							
H_2	U	U	U	U	15.03	9.12	17.76
CH_4	U	U	U	0.94	1.62	2.42	2.61
C_2H_2	0.06	U	0.13	0.06	U	0.23	U
C_2H_6	0.20	U	0.11	0.05	0.13	U	U
3 Stages							
H_2	U	U	U	U	5.94	14.57	17.80
CH_4	0.09	U	0.16	0.16	1.43	2.26	2.69
C_2H_2	U	0.08	0.11	0.12	0.02	0.11	0.09
C_2H_6	0.59	U	0.34	U	1.41	U	U
4 Stages							
H_2	U	U	U	U	U	37.48	U
CH_4	U	0.03	U	U	0.98	1.63	1.12
C_2H_2	U	0.04	0.48	U	U	U	0.14
C_2H_6	U	0.10	0.25	U	U	U	0.12

U = undetectable due to lower than detected limit

electric field strength as shown in Figure 4.11, promoting higher average electron energy, which in turn increases the conversions. Morinaga and Suzuki (1962) also found that, with a fixed geometry, the quantity of electricity transferred between electrodes increased as the applied voltage increased. An increase in the stage number of reactors in operation resulted in increasing both conversions of ethylene and oxygen since the system has a longer residence time leading to electrons having more chance to break down C_2H_4 and O_2 molecules.

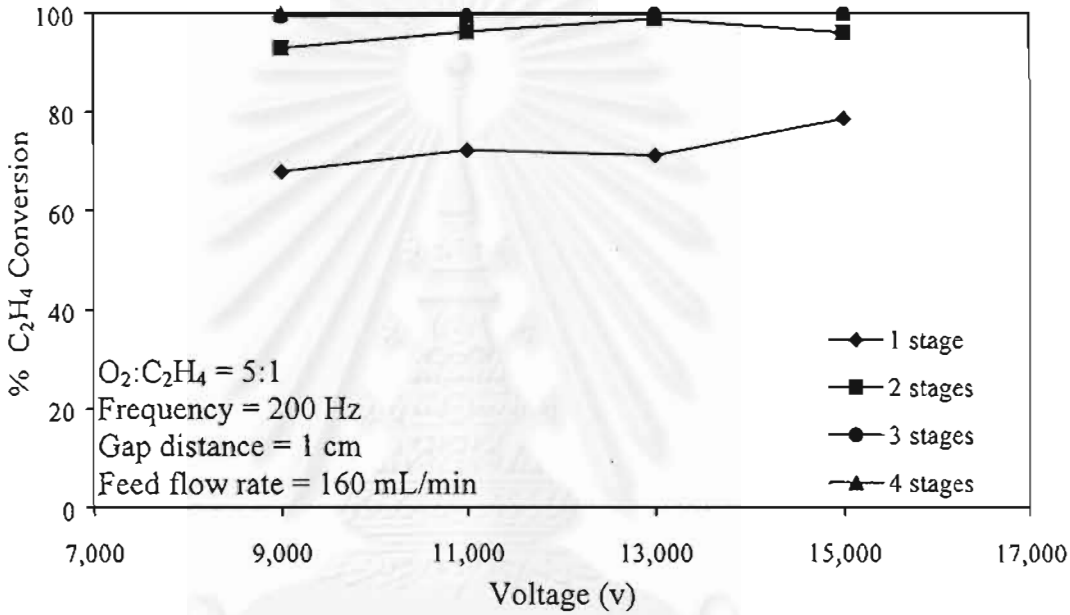

Figure 4.9 Effect of applied voltage on C_2H_4 conversion at different stage number of reactors.

4.3.2 Effects on Product Selectivities

The effects of applied voltage on CO and CO_2 selectivities are shown in Figures 4.12 and 4.13, respectively. As the applied voltage increased, the CO_2 selectivity increased whereas the CO selectivity decreased. This is because increasing voltage results in increasing current as shown in Figure 4.11. As a result, there are more oxygen active species available to oxidize CO molecules leading to higher CO_2 selectivity. For any given applied voltage, the CO selectivity decreased while the CO_2 selectivity increased when the gas mixture was passed through a higher stage number of plasma reactors. The reason is that a higher number of multi-

stage plasma reactors increases the residence time of the gases. Consequently, the oxidation reaction increases.

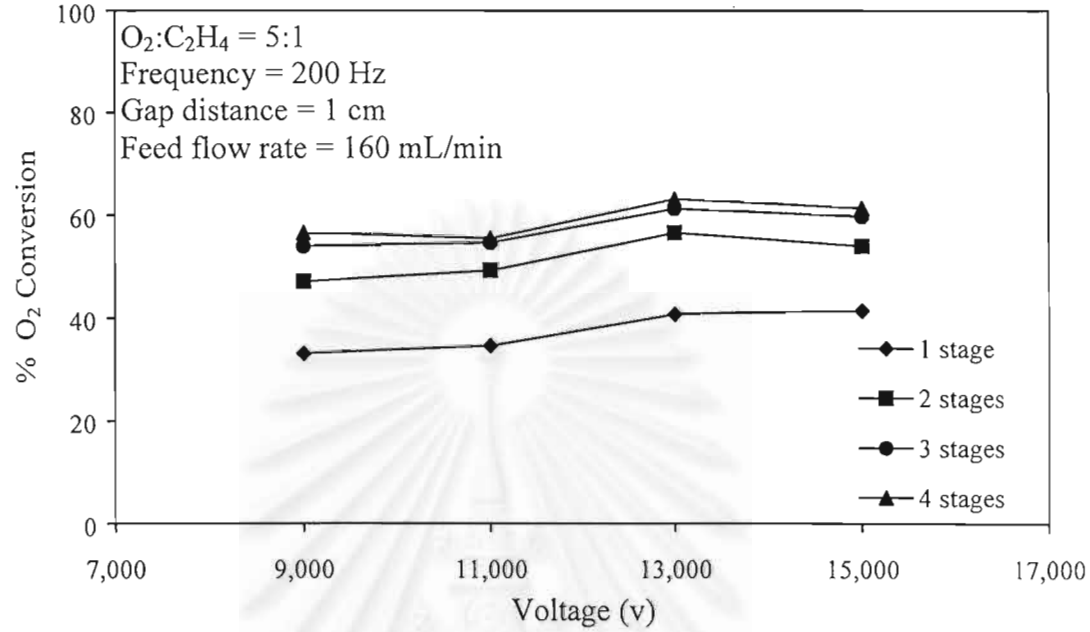

Figure 4.10 Effect of applied voltage on O_2 conversion at different stage number of reactors.

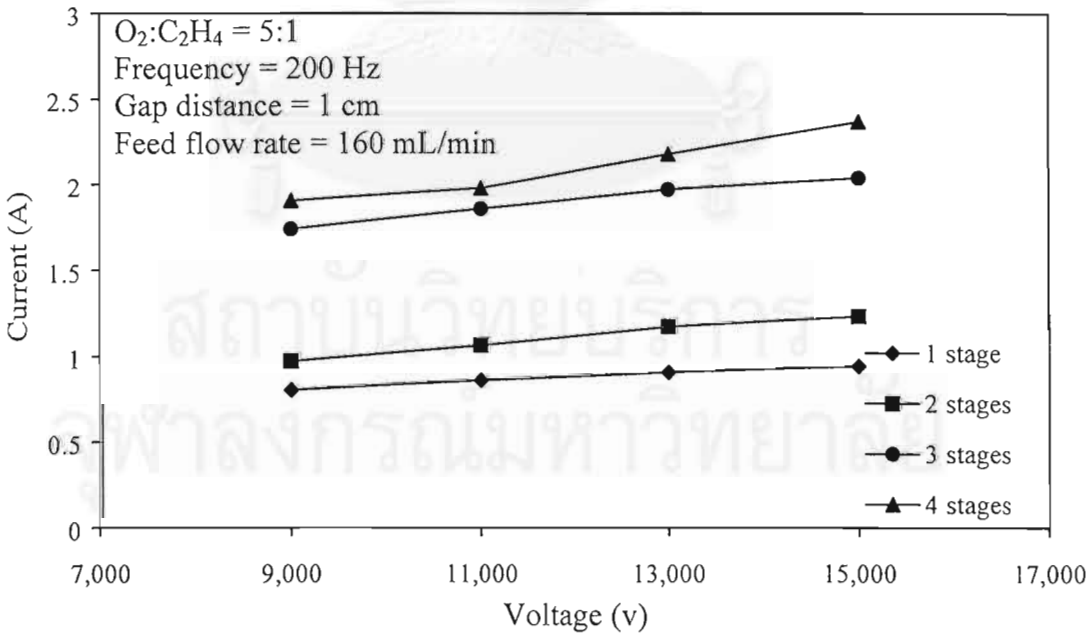

Figure 4.11 Effect of applied voltage on current at different stage number of reactors.

In this study, 11,000 V was selected for next experiments because a higher applied voltage than 11,000 V resulted in higher by-product selectivities (see Table 4.2). Even though the system at 9,000 V had less by-product selectivities than at 11,000 V but the C_2H_4 conversion was lower than at 11,000 V.

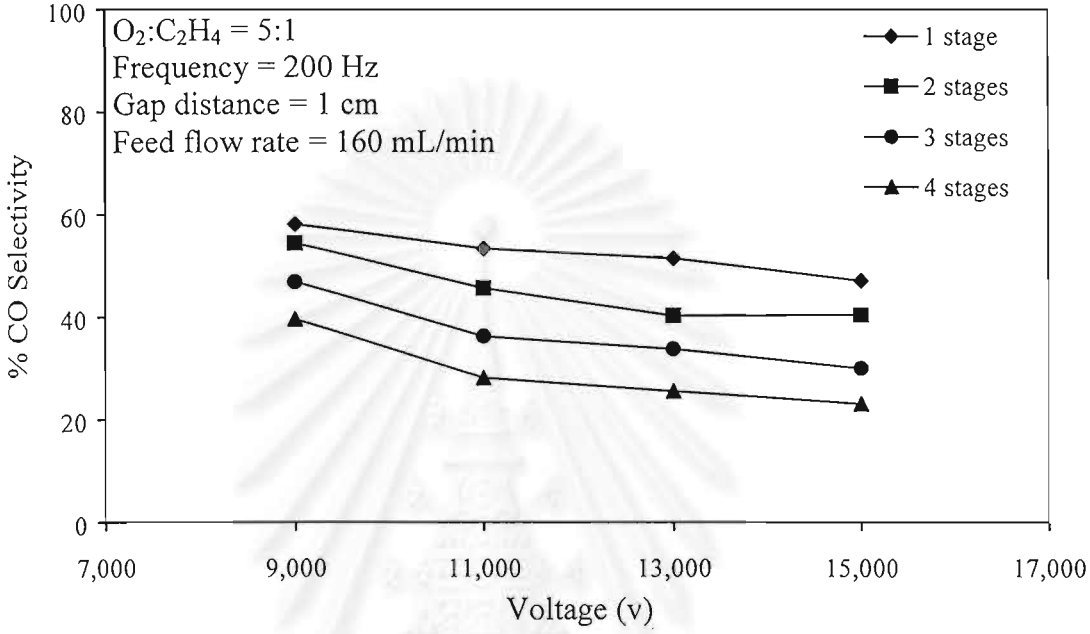

Figure 4.12 Effect of applied voltage on CO selectivity at different stage number of reactors.

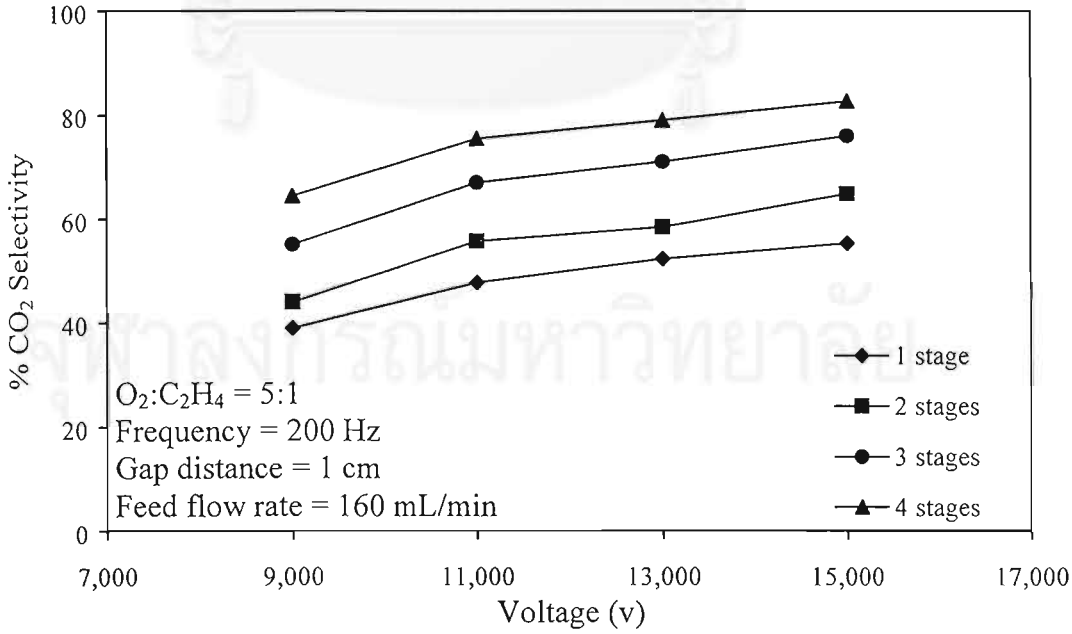

Figure 4.13 Effect of applied voltage on CO_2 selectivity at different stage number of reactors.

Table 4.2 Effect of applied voltage on by-product selectivities at a feed flow rate of 160 mL/min, 200 Hz, and a gap distance of 1 cm with different stage number of reactors

Types of by-products	% Selectivities			
	Applied Voltage, V			
	9000	11,000	13,000	15,000
1 Stage				
H_2	U	U	U	U
CH_4	U	U	0.29	U
C_2H_2	U	0.26	0.09	0.25
C_2H_6	U	U	U	0.15
2 Stages				
H_2	U	U	U	U
CH_4	0.36	U	0.10	U
C_2H_2	U	0.13	0.52	U
C_2H_6	U	0.11	0.65	0.06
3 Stages				
H_2	U	U	U	U
CH_4	0.08	0.19	U	U
C_2H_2	U	0.11	0.01	0.09
C_2H_6	U	0.34	0.08	0.03
4 Stages				
H_2	U	U	U	U
CH_4	0.14	U	U	U
C_2H_2	U	0.48	0.23	U
C_2H_6	U	0.25	0.08	0.08

U = undetectable due to lower than detected limit

4.4 Effects of Feed Flow Rate

4.4.1 Effects on Ethylene and Oxygen Conversions

Figures 4.14 and 4.15 illustrate the effects of feed flow rate on C_2H_4 and O_2 conversions, respectively. For either a single or two-stage system, both C_2H_4 and O_2 conversions decreased with increasing the feed flow rate in the studied range of 40 to 240 ml/min because an increase in the feed flow rate corresponds to a decrease in the residence time. For any given feed flow rate, a higher stage number of plasma reactors in use resulted in higher conversions of both C_2H_4 and O_2. With a decrease in the feed flow rate or an increase in the stage number of plasma reactors in operation, electrons have more possibility to collide with C_2H_4 and O_2 molecules leading to higher conversions of both reactants.

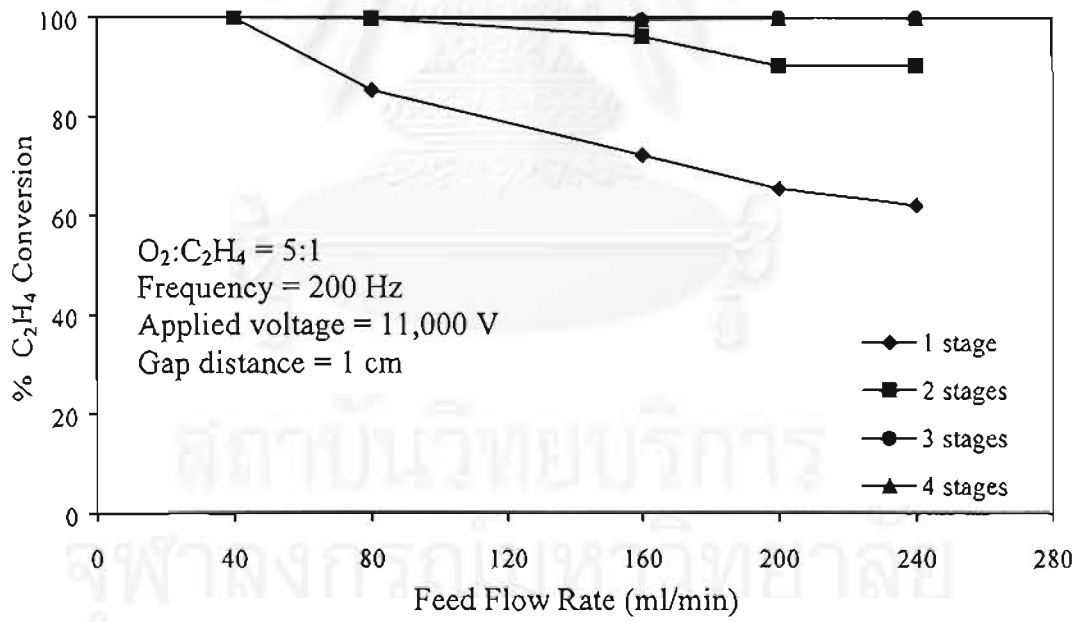

Figure 4.14 Effect of feed flow rate on the C_2H_4 conversion at different stage numbers of reactors.

4.4.2 Effects on Product Selectivities

The effects of feed flow rate on CO and CO_2 selectivities are shown in Figures 4.16 and 4.17, respectively. For any given stage number, the CO selectivity increased with increasing the feed flow rate while the opposite trend was observed for the CO_2 selectivity. A higher gas flow rate or a lower of stage number reduces the opportunity of collision between electrons and O_2 molecules. Therefore, the oxidation of CO is reduced resulting in lower CO_2 formation.

As shown in Table 4.3, an increase in feed flow rate results in increasing byproduct selectivities. Interestingly, at the lowest feed flow rate of 40 mL/min, by-products were not found and the complete C_2H_4 conversion was observed (see Figure 4.14). Regarding to the air pollution control, one should select this lowest flow rate of 40 mL/min. However, this condition gives the complete oxidation of ethylene which cannot observe any process parameters. Thus, a feed flow rate of 160 mL/min was selected for further study in order to determine the other effects such as stage number and the presence of photocatalyst.

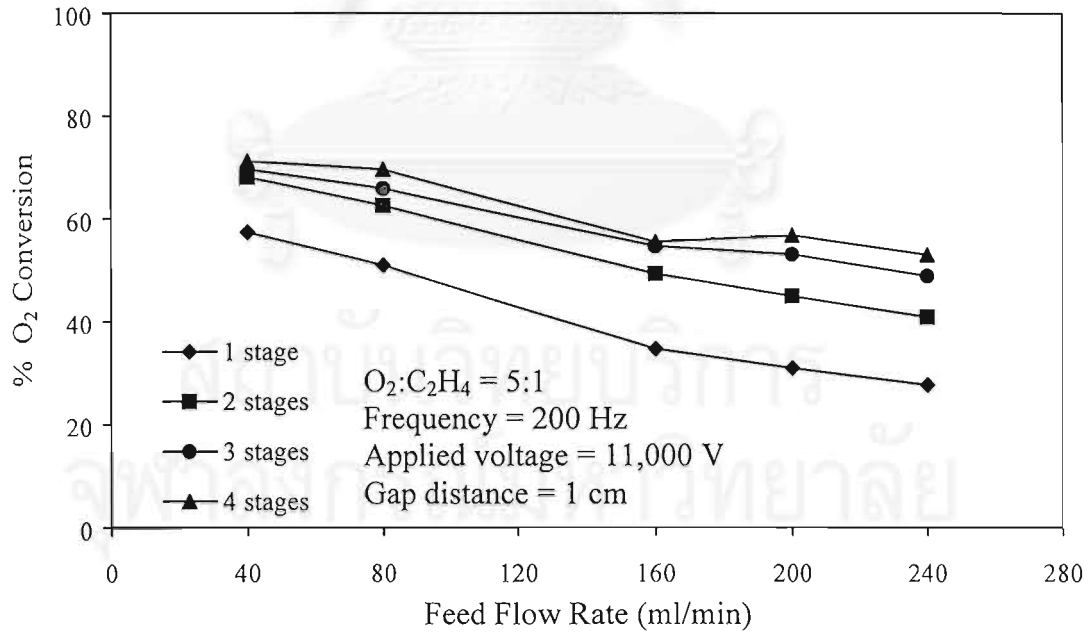

Figure 4.15 Effect of feed flow rate on O_2 conversion at different stage numbers of reactors.

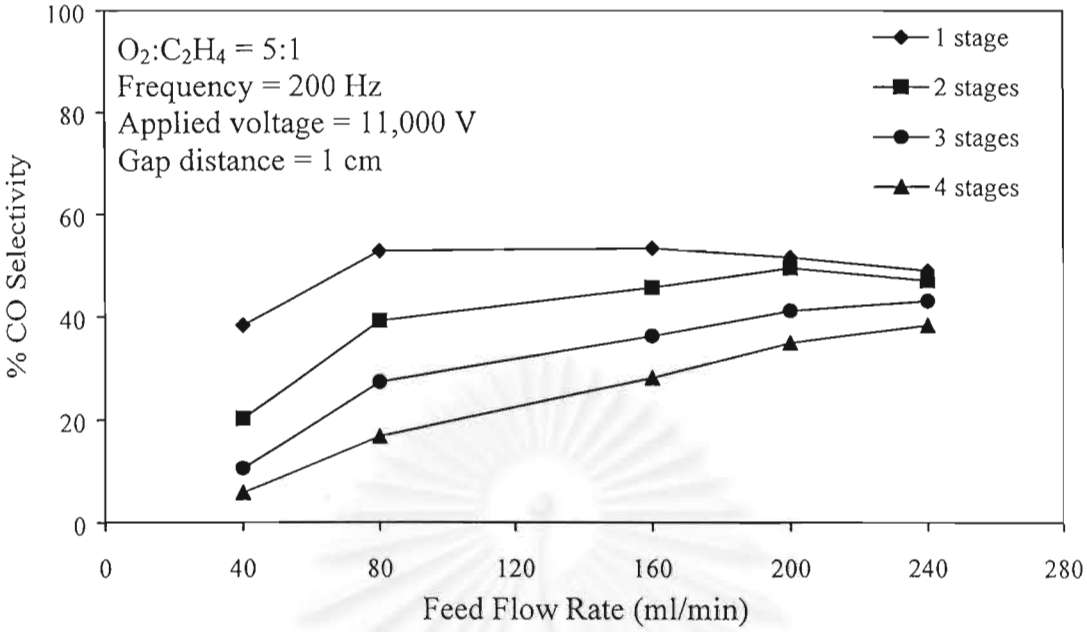

Figure 4.16 Effect of feed flow rate on CO selectivity at different stage numbers of reactors.

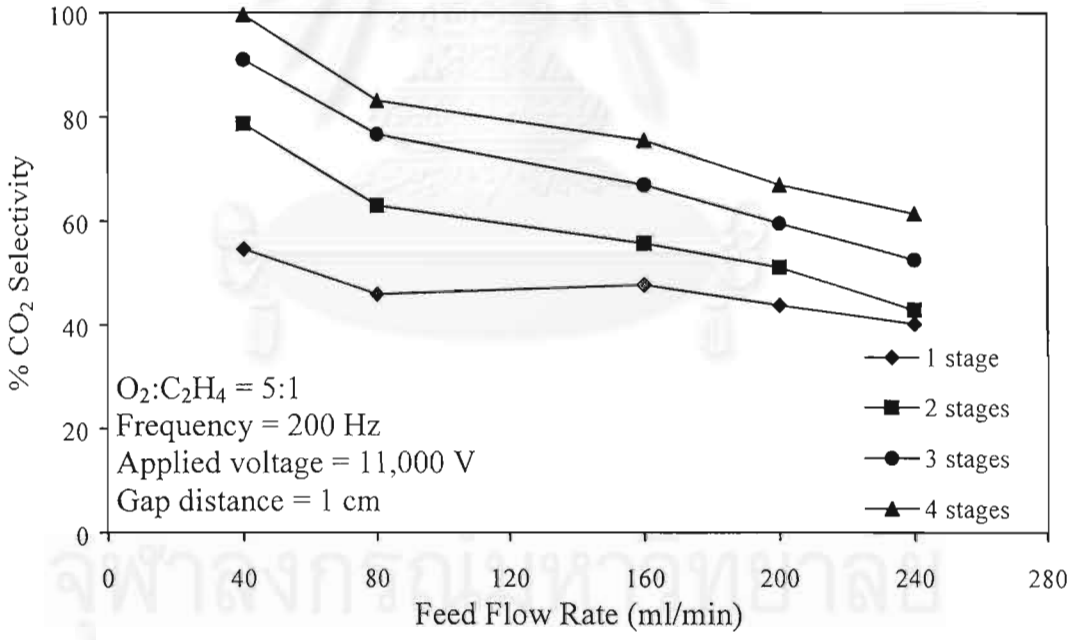

Figure 4.17 Effect of feed flow rate on CO_2 selectivity at different stage numbers of reactors

.

Table 4.3 Effect of feed flow rate on by-product selectivities at 11,000 V, 200 Hz, and a gap distance of 1 cm with different stage numbers of reactors

Types of by-products	% Selectivities				
	Feed Flow Rate, mL/min				
	40	80	160	200	240
1 Stage					
H_2	U	U	U	U	U
CH_4	U	0.22	U	0.65	0.19
C_2H_2	U	0.39	0.26	0.45	U
C_2H_6	U	0.39	U	0.24	0.25
2 Stages					
H_2	U	U	U	U	U
CH_4	U	0.03	U	0.05	0.38
C_2H_2	U	0.10	0.13	0.13	0.19
C_2H_6	U	0.38	0.11	0.07	0.39
3 Stages					
H_2	U	U	U	U	U
CH_4	U	0.05	0.19	U	0.03
C_2H_2	U	0.19	0.11	0.19	0.28
C_2H_6	U	0.18	0.34	0.51	0.27
4 Stages					
H_2	U	U	U	U	U
CH_4	U	0.17	U	U	0.09
C_2H_2	U	U	0.48	0.05	U
C_2H_6	U	0.19	0.25	0.02	0.18

U = undetectable due to lower than detected limit

4.5 Effects of Stage Numbers of Plasma Reactors

4.5.1 Effects on Ethylene and Oxygen Conversions

Figure 4.18 shows the effect of stage number of plasma reactors on the C_2H_4 conversion. Under the studied conditions, complete conversion of C_2H_4 was observed at two residence times of 1 and 0.75 sec. The residence time calculated is based on the reaction volume between two electrodes. For any given flow rate, the residence time of the system is calculated by multiplying a stage number to the residence time of single stage. As expected, at the lowest residence time of 0.38 sec, the conversion of C_2H_4 increased with increasing number of stage. As seen from Figure 4.19, for any given residence time, an increase in stage number seems not to affect the oxygen conversion. The result can be explained that the system was operated under the excess oxygen environment.

4.5.2 Effects on Product Selectivities

The effects of the stage number on the CO and CO_2 selectivities are shown in Figures 4.20 and 4.21, respectively. For any given residence time, as the stage number of the plasma reactors increased, the CO_2 selectivity increased whereas the CO selectivity decreased. It can be explained that a higher stage number can enhance the collision between electrons and O_2 molecules; therefore, the oxidation of CO is increased resulting in the higher CO_2 formation.

4.6 Effects of the Presence of Different Photocatalysts

4.6.1 Glass Ring Support

4.6.1.1 Effecst on Ethylene and Oxygen Conversions

Table 4.4 shows the effect of two types of TiO_2 coated on glass ring on C_2H_4 and O_2 conversions. It appears that both Degussa P25 and Sol-Gel TiO_2 did not significantly enhance both C_2H_4 and O_2 conversions, which are consistent to the result reported that by Harndumrongsak *et al.* (2002).

4.6.1.2 Effects on Product Selectivities

As can be seen from Table 4.4, both CO and CO_2 selectivities are not affected by the presence of either Degussa P25 or sol-gel TiO_2. The result of the present study is different from the previous work (Harndumrongsak *et al.*, 2002),

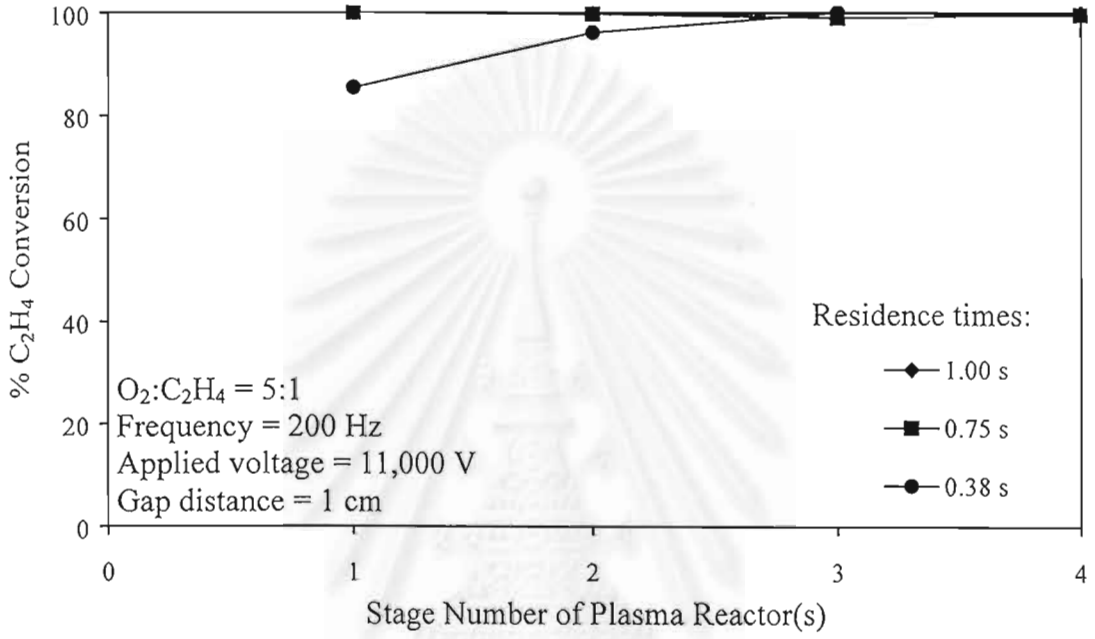

Figure 4.18 Effect of stage number on C_2H_4 conversion at different residence times

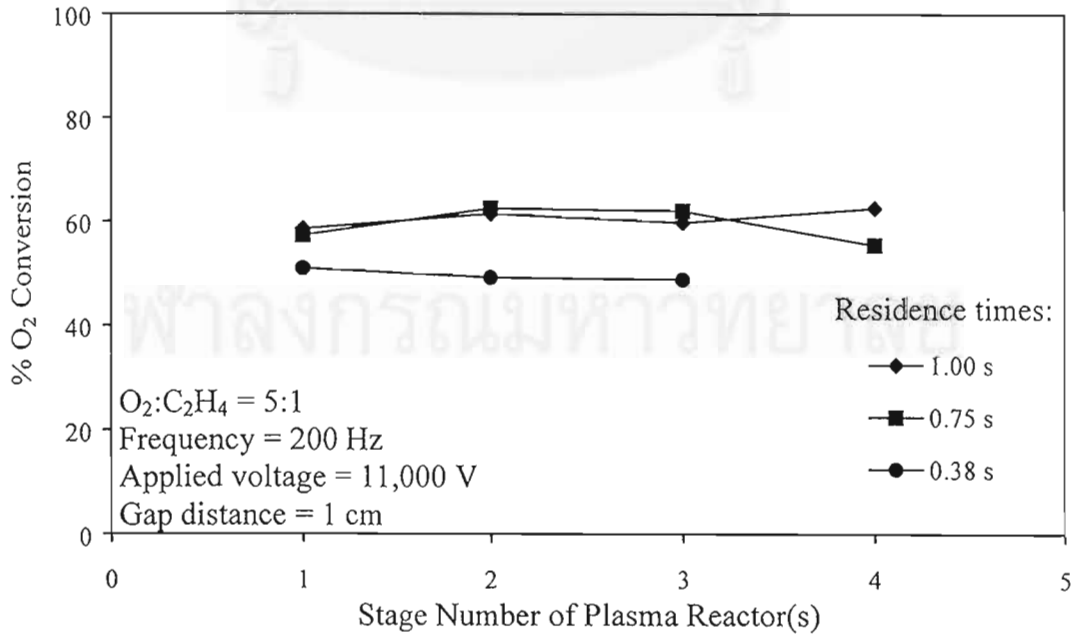

Figure 4.19 Effect of stage number on O_2 conversion at different residence times

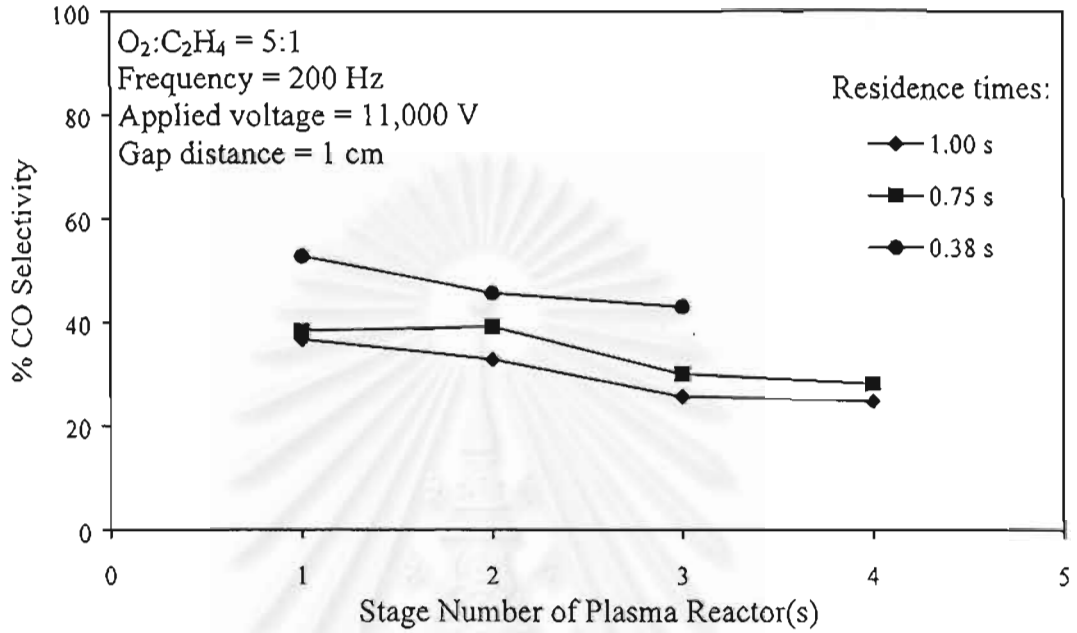

Figure 4.20 Effect of stage number on CO selectivity at different residence times

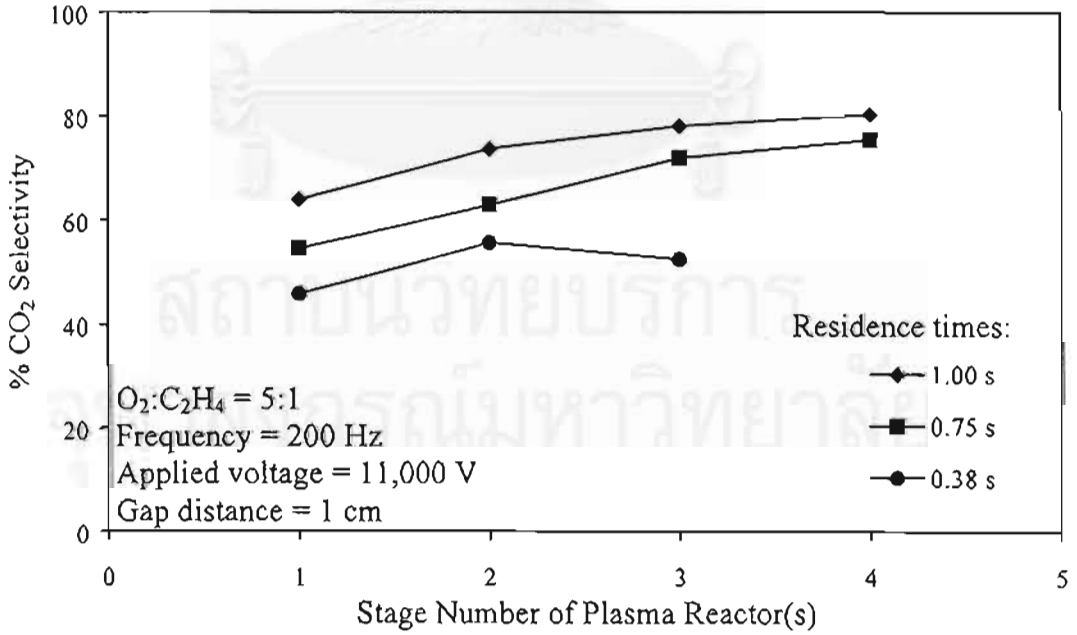

Figure 4.21 Effect of stage number on CO_2 selectivity at different residence times

Table 4.4 Effect of Photocatalysts coated on glass ring at a flow rate of 160 ml/min, 11,000 V, a gap distance of 1 cm, and weight of photocatalyst of 0.008 g

Stage(s)	Frequency = 200 Hz				Frequency = 50 Hz			
	% Conversion		% Selectivity		% Conversion		% Selectivity	
	O_2	C_2H_4	CO	CO_2	O_2	C_2H_4	CO	CO_2
No catalyst								
1	30	61	29	42	45	82	13	86
2	44	87	54	49	56	98	14	90
3	52	98	45	60	59	100	8	96
4	56	100	34	71	60	100	6	98
Degussa P25								
1	28	58	56	38	45	79	13	85
2	43	85	54	44	61	98	14	87
3	51	98	45	54	64	100	8	94
4	56	100	36	64	65	100	6	96
Sol-Gel TiO_2								
1	28	58	59	42	53	87	13	88
2	42	86	54	46	60	93	11	90
3	51	97	46	56	62	100	7	93
4	55	100	36	67	62	100	6	94

in which glass wool was used instead of a glass ring. From the previous work, the addition of TiO_2 increased the CO_2 selectivity from 58 to 71 % at the power of 3.5 W and decreased the CO selectivity. A possible explanation is that the glass ring used has less surface area than the glass wool. With the low surface area of the glass ring, it had to be coated eight times to obtain the same amount of TiO_2 on the glass wool. As a result, a multilayer of TiO_2 was formed on the glass ring. On the contrary, the glass wool only required one coating for the same amount of TiO_2 to deposit. It has

been known that an external thin layer of TiO_2 exposed to light can initiate redox reaction. That is why the TiO_2-coated glass ring did not have the same effect on the selectivity as the glass wool. Another reason could be the location of the glass ring, which was far from the plasma zone so the light generated from plasma could not activate the catalyst effectively.

4.6.2 Glass Wool Support

4.6.2.1 Effects on Ethylene and Oxygen Conversions

Table 4.5 shows the effects of the presence of different photocatalysts coated on glass wool on conversions and product selectivities. In comparison to the absence of photocatalyst all of Degussa P25, sol-gel TiO_2 and 1%Pt/sol-gel TiO_2 significantly increased the C_2H_4 conversion by 20% and 10% with 1 and 2 stages in operation, respectively. However, the same effect was not observed when higher than two stages were used since the ethylene conversion on all catalysts approached 100%. The presence of all studied photocatalysts appeared to increase the O_2 conversion in a following order: 1%Pt/sol-gel TiO_2 >sol-gel TiO_2 >Degussa P25 for any given stage number. The results imply that the energy released from the plasma will excite TiO_2 to create the energy band gap of conductance band and valance band leading to the oxidation and reduction reactions on the TiO_2 surface.

4.6.2.2 Effects on Product Selectivities

During plasma generation, it also releases the energy that can activate TiO_2; therefore, the catalyst can promote more complete oxidation of C_2H_4. The presence of either sol-gel TiO_2 or the commercial TiO_2 (Degussa P25) increased the CO_2 selectivity by 4-7%, but decreased the CO selectivity by 6%. With 1%Pt loaded on sol-gel TiO_2, the CO_2 selectivity increased significantly about 10-17%. Since Pt on TiO_2 attributes to the acceleration of superoxide radical anion, $O_2^{\bullet-}$, formation and consequently decreases the recombination process leading to enhance the catalytic activity (Blazkova *et al.*, 1998).

During plasma generation, it is believed to generate UV light. Under the studied conditions of frequency 200 Hz, voltage 9,000 V, and a gap distance of 1 cm, the UV intensity generated from the first-stage reactor was measured to be about

0.012 μW/cm^2 or 3.3943 μW by using a UV meter as shown in Figure 4.22. As compared to the input power of 97 W, the UV intensity was considerably small. However, the UV light meter is only to measure the light intensity in the UV range but the energy released from plasma has also in various wavelengths. In addition to UV, shorter wavelengths can also initiate the photocatalytic reaction. From the results, it can be concluded that ethylene is dominantly decomposed by plasma while a minor effect from photocatalysis was observed.

Tables 4.5 Effect of Photocatalyst coated on glass wool at a flow rate of 160 mL/min, 200 Hz, 9,000 V, a gap distance of 1 cm, and weight of photocatalyst = 0.008 g

Types of catalyst	Stage(s)	% Conversion		% Selectivity	
		C_2H_4	O_2	CO	CO_2
No catalyst	1	47	22	70	29
	2	80	37	61	35
	3	95	47	52	46
	4	99	52	43	56
Degussa P25	1	67	30	58	36
	2	90	43	56	42
	3	98	50	48	51
	4	99	53	41	60
Sol-Gel TiO_2	1	68	33	57	38
	2	90	44	55	43
	3	99	50	48	51
	4	99	54	41	60
1% Pt/Sol-Gel TiO_2	1	68	35	56	46
	2	90	46	55	46
	3	98	53	46	56
	4	99	57	35	70

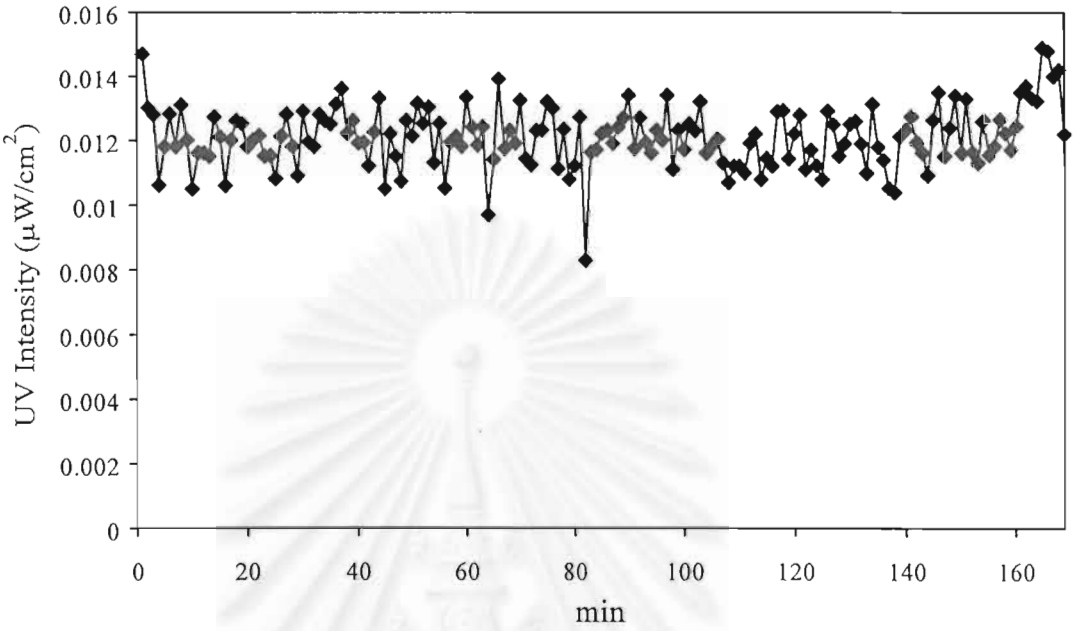

Figure 4.22 The UV light intensity generated from the first-stage plasma reactor operated at a feed flow rate of 160 mL/min, 200 Hz, 9,000 V, and a gap distance of 1 cm.

CHAPTER V
CONCLUSIONS AND RECOMMENDATIONS

5.1 Conclusions

Under the studied conditions with and without photocatalysts, ethylene was almost completely removed by the corona discharge. The ethylene decomposition efficiency decreased with increasing frequency. Since at a higher frequency, current is lowered leading to the reduction of the number of electrons generated. A higher applied voltage increased the C_2H_4 and O_2 conversions as well as CO_2 selectivity since current is increased with increasing applied voltage. A higher feed flow rate decreased both C_2H_4 and O_2 conversions and CO_2 selectivity because of decreasing residence time. For any given residence time, an increase in stage number of the sole plasma system enhanced remarkably the ethylene oxidation reaction. The presence of catalyst coated on glass ring did not affect significantly C_2H_4 and O_2 conversions and CO_2 selectivity. In case of coating on glass wool, both Degussa P25 and TiO_2 prepared by sol-gel method increased C_2H_4 and O_2 conversions and CO_2 selectivity because the energy produced from plasma generation activates TiO_2 to promote complete oxidation reaction. Interestingly, the presence of 1%Pt on TiO_2 increased significantly the CO_2 selectivity as compared to blank Degussa P25 and blank sol-gel TiO_2 since Pt accelerates the formation of superoxide radical anion, $O_2^{\bullet-}$, and decreases the recombination process.

5.2 Recommendations

Air should be used instead of pure oxygen in order to reduce the treatment cost. VOCs should be investigated using the present plasma system with and without catalyst. Other types of catalysts and supports are highly recommended to study for this application.

REFERENCES

Blazkova, A., Csolleova, I,. and Brezova, V. (1998). Effect of Light Sources on the Phenol Degradation using Pt/TiO2 Photocatalysts Immobilized on Glass Fibers. Journal of Photochemistry and Photobiology A: Chemistry, 113, 251-256.

Cheng, Y. (1996). Kinetic and Mechanistic Studies of Volatile Organic Compound Oxidation Catalysis Using Thin Film Model Pt Catalysts. A Research Proposal Submitted in partial Fulfillment of The Preliminary Examination Requirements, The University of Michigan.

De Lasa, H.I., Dogu, G., and Ravella, A. (Eds.). (1992). Chemical Reactor Technology for Environmentally Safe Reactors and Product. Dordrecht/Boston/London: Kluwer Academic Publishers, 577-608.

De Nevers N. (1995). Air Pollution Control Engineering. International Editions. New York: McGRAW-HILL.

Einaga, H., Futamura, S., and Ibusuki, T. (2001). Complete Oxidation of Benzene in Gas Phase by Platinized Titania Photocatalysts. Environmental Science & Technology, 35(9), 1880-1884.

Eliasson, B., Hirth, M., and Kogeischatz, U. (1987). Ozone Synthesis from Oxygen in Dielectric Barrier Discharge. Journal of Applied Physics, 20, 1421-1437.

Eliasson, B. and Kogeischatz, U. (1991). Nonequilibrium Volume Plasma Chemical Processing. IEEE Transactions on Plasma Science, 19(6), 1063-1077.

Futamura, S. and Yamamoto, T. (1997). Byproduct Identification and Mechanism Determination in Plasma Chemical Decomposition of Trichloroethylene. IEEE Transactions on Industry Applications. , 33(2), 447-453.

Futamura, S., Zhang, A., and Yamamoto, T. (1999). Mechanisms for Formation of Inorganic Byproducts in Plasma Chemical Processing of Hazardous Air Pollutants. IEEE Transactions on Industry Applications. 35(4), 760-766.

Futamura, S., Einaga, H., and Zhang, A. (2001). Comparison of Reactor Performance in the Nonthermal Plasma Chemical Processing of Hazardous Air Pollutants. IEEE Transactions on Industry Applications, 37(4), 978-985.

Grill, A. (1994). Cold Plasma in Materials Fabrication: From Fundamentals to

Applications. IEEE Press: New York.

Harndumrongsak, B. (2002). Oxidation of Ethylene in a Plasma Environment. M.Sc.,Thesis, Chulalongkorn University, Bangkok.

Harndumrongsak, B., Lobban, L.L., Rangsunvigit, P., and Kitiyanan, B. (2002). Oxidation of Ethylene in Plasma Environment. Proceeding of the 9th APCChE Congress in Christchurch, New Zealand, 29 September – 3 October 2002.

Herrmann, J.-M. (1999). Heterogeneous Photocatalysis: Fundamentals and Applications to the Removal of Various Types of Aqueous Pollutant. Catalysis Today, 53, 155-129.

Hill, B.J. Master Thesis, University of Oklahoma, 1997.

Huang, A., Xia, G., Wang, J., Suib, S.L., Hayashi, Y., and Hiroshige, M. (2000). CO_2 Reforming of CH_4 by Atmospheric Pressure AC Discharge Plasmas. Journal of Catalysis, 189, 349-359.

Huang, L., Nakajyo, K., Hari, T., Ozawa, S., and Matsuda, H. (2001). Decomposition of Carbon Tetrachloride by a Pulsed Corona Reactor incorporated with in situ Absorption. Industrial and Engineering Chemistry Research, 40, 5481-5486.

Kruapong, A. (2000). Partial Oxidation of Methane to Synthesis Gas in Low Temperature Plasmas. M.Sc., Thesis, Chulalongkorn University, Bangkok.

Litter, M.I. (1999). Heterogeneous Photocatalysis Transition Metal Ions in Photocatalytic Systems. Applied Catalysis B: Environmental, 13, 89-114.

Liu, C., A. Marafee, B. Hill, G. Xu, R. Mallinson, and L. Lobban, (1996). "Oxidative Coupling of Methane with AC and DC Corona Discharge," Ind. Eng. Chem. Res., 35, 3295.

Malik, M.A. and Malik, S.A. (1999). Catalyst Enhanced oxidation of VOCs and Mathane in Cold-Plasma Reactors. Platinum Metal Review, 43(3), 109-113.

Morinaga, K., Suzuki, M. *Bull. Chem.* Soc. of Japan. 1961, 34(2), 157-161.

Morinaga, K., Suzuki, M. *Bull. Chem.* Soc. of Japan. 1962, 35(2), 204-207.

Nakamura, I., Negishi, N., Kutsuna, S., Ihara, T., Sugihara, S., and Takeuchi, K. (2000). Role of Oxygen Vacancy in the Plasma-treated TiO_2 Photocatalyst

with Visible Light Activity for NO Removal. Journal of Molecular Catalyst A: Chemical, 161, 205-212.

Nasser, E. (1971). Fundamentals of Gaseous Ionization and Plasma Electronics, USA: John Wiley & Sons, Inc.

Obuchi, E., Sakamoto, T., and Nakano, K. (1999). Photocatalytic Decomposition of Acetaldehyde over TiO_2/SiO_2 Catalyst. Chemical Engineering Science, 57, 1525-1530.

Papaethimiou, P., Ioanides, T., and Verykios, X.E. (1997). Combustion of Non-halogenated Volatile Organic Compounds over Group VIII Metal Catalysts. Applied Catalysis B: Environmental, 13, 175-184.

Peral, J., Domenech, X., and Ollis, D.F. (1997). Heterogeneous Photocatalyst for Purification, Decontamination and Deodorization of Air. Journal of Chemical Technology and Biotechnology, 70, 117-140.

Robertson, P.K.J. (1996). Semiconductor Photocatalysis: An Environmentally Acceptable Alternative Production Technique and Effluent Treatment Process. Journal of Cleaner Production, 4:3-4, 203-212.

Rosacha, L.A., Anderson, G.K., Bechtold, L.A., Coogan, J.J., Heck, H.G., Kang, M., McCulla, W.H., Tennant, R.A., and Wantuck, P.J. (1993). Treatment of Hazardous Organic Wastes using Silent Discharge Plasmas. Non-Thermal Plasma Technique for Pollution Control., NATO ASI series, 34, part B, 128-139.

Sano, N., Nagamoto, T., Tamon, H., Suzuki, T., and Okazaki, M. (1997). Removal of Acetaldehyde and Skatole in Gas by a Corona-Discharge Reactor. Industrial & Engineering Chemistry Research, 36, 3783-3791.

Sutthiruangwong, S. (1999). Plasma catalytic production of methanol. M.Sc., Thesis, Chulalongkorn University, Bangkok.

Thanyachotpaiboon, K., Chavadej, S., Caldwell, L., Lobban, L.L., and Mallinson, R.G. (1998). Conversion of methane to Higher Hydrocarbons in AC Nonequilibrium Plasmas. AIChE Journal, 44(10), 2252-2257.

Tsai, C.H., Lee, W.J., Chen, C.Y., and Liao, W.T. (2001). Decomposition of CH_3SH in a RF Plasma Reactor: Reaction Products and Mechanisms. Industrial & Engineering Chemistry Research 40, 2384 –2395.

Zhang, J., Ayusawa, T., Minagawa, M., Kinugawa, K., Yamashita, H., Matsuoka, M., and Anpo, M. (2001). Investigations of TiO_2 Photocatalysts for the Docomposition of NO in the Flow System. Journal of Catalysis, 198, 1-8.

APPENDICES

Appendix A: Assumptions, Definitions, and Calculations

In this work, the following assumptions are made:

1. All the gaseous behaviors obey the ideal gas law
2. The change in the system, pressure is very small and negligible.
3. The pressure in the system equals the atmospheric pressure (1 atm)

The total molar flow rate of the gaseous stream can be determined from the following equation:

$$N = q \times (P/RT) \qquad \text{(B.1)}$$

where

q = total volumetric flow rate

P = total pressure of the system

R = gas constant (82.051 atm·ml·mol^{-1}·min^{-1}·K)

T = absolute ambient temperature (K)

The molar flow rate of each component can be obtained by multiplying its fraction derived from the gas chromatography analysis by the total molar flow rate.

The conversion is defined as:

$$\% \text{ Conversion} = \frac{\text{Mole reactant in} - \text{Mole reactant out}}{\text{Mole reactant in}} \times 100 \qquad \text{(B.2)}$$

The first selectivity is defined as:

$$\% \text{ Selectivity} = \frac{P \times \text{Mole of } C_p \text{ produced}}{R \times \text{Mole of } C_R \text{ converted}} \times 100 \qquad \text{(B.3)}$$

where

P = number of carbon atoms in product

R = number of carbon atoms in reactant

C_p = product that has carbon P atom

C_R = reactant that has carbon R atom

The second selectivity is defined as:

$$\% \text{ Selectivity} = \frac{\text{Mole of product}}{\text{Total mole of all products}} \times 100 \qquad \text{(B.4)}$$

To determine the energy efficiency of corona discharge system, the specific energy consumption was calculated in a unit of electron-volt per molecule of converted carbon (eV/m_c) from the following equation:

$$\text{Specific energy consumption} = \frac{P \times 60}{(1.602 \times 10^{-19}) \times \tilde{N} \times M_C} \quad eV/\text{ mol } C_2H_4$$

where P = Power (W)

$\tilde{N}$ = Avogadro's number = 6.02×10^{23} molecules.g-mole^{-1}

M_C = Rate of carbon in feed gas converted (g-mole.min^{-1})

1 eV = 1.602×10^{-19} Ws

To determine the UV light intensity of corona discharge system, the intensity was calculated in a unit of μW. In this work, the following assumption was that the UV light spread out in all direction.

$$\text{Intensity } (\mu W) = \frac{\text{Intensity measured from UV meter } (\mu W/cm^2)}{\text{Area of sphere } (cm^2)}$$

Where Area of sphere = $4\pi r^2$

r = 1.5 cm

PIM-1

Tomorrows Technology

PROGRAM AT GLANCE

FIRST INTERNATIONAL SYMPOSIUM ON

PROCESS INTENSIFICATION & MINIATURISATION

IN BIOLOGICAL, CHEMICAL, ENVIRONMENTAL AND ENERGY CONVERSION TECHNOLOGIES

18 - 21 August 2003

Organized by:

University of Newcastle upon Tyne

Co-organized by:

One NorthEast

the institute of energy

BIOMASS ENERGY

http://www.ncl.ac.uk/pimsym

TECHNICAL PROGRAM IN BRIEF

	Monday August 18, 2003	Tuesday August 19, 2003	Wednesday August 20, 2003	Thursday August 21, 2003
REGISTRATION	Foyer A 8:30-9:30			
(OWR)	Room A 9:30-10:00			
Plenary	Room A 10:00-10:40			
Workshop-I	Room A 11:00-17:40			
BioTech-I	Room B 11:00-12:40			
Separation-I	Room B 14:00-15:40			
BioTis	Room B 16:00-17:40			
BioTech-II		Room A 9:00-10:10		
Keynote		Room A 10:10-10:40		
Separation-II		Room B 9:00-10:40		
Microreactors-I		Room A 11:00-12:40		
Env. Tech.-I		Room B 11:00-12:40		
Energy-I		Room A 14:00-15:40		
Workshop-II		Room B 14:00-17:30		
Energy-II		Room A 16:00-17:40		
Microreactors-II			Room A 9:00-10:40	
Particle Tech.			Room B 9:00-10:40	
Chemical Reactor-I			Room A 11:00-12:40	
Env. Tech.-II			Room B 11:00-12:40	
Chemical Reactor-II			Room A 14:00-15:40	
Env. Tech.-III			Room B 14:00-15:40	
Catalysis			Room A 16:00-17:40	
Env. Tech.-IV			Room B 16:00-17:40	
Open Forum- Discussion			Room A 17:40-18:30	
Chemical Reactor-III				Room B 9:00-10:40
Uni. Lab Visit - Closing				University 11:00-12:40
Ref. Break (Morning)	10:40 – 11:00	10:40 – 11:00	10:40 – 11:00	10:40 – 11:00
Ref. Break (Afternoon)	15:40 – 16:00	15:40 – 16:00	15:40 – 16:00	
Lunches	12:40 - 14:00	12:40 - 14:00	12:40 - 14:00	
Welcoming Reception	19:30 - 22.30			
Symposium Banquet		19:30 – 22.30		

MINIATURIASATION OF ESTERIFICATION REACTION USING NOVEL CATALYST (AMBERLYST- 15 & HYDROGEN PEROXIDE), Mrs. S. D. Garway, Dr. S. S. Bhagade, Mr. R. Kulkarni, Laxminarayan Institute of Technology Nagpur , University of Birmingham, UK (on page 58)

OXIDATIVE REMOVAL OF ETHYLENE BY A MULTISTAGE PLASMA REACTOR IN THE PRESENCE OF SOL-GEL TiO_2, K. Saktrakool, S. Chavadej, P. Rangsunvigit, and Lance L. Lobban, Chulalongkorn University, Thailand, The University of Oklahoma, USA (on page 59)

A SOLVENT SCREENING MODEL FOR DISSOCIATIVE EXTRACTIVE CRYSTALLIZATION, A. Lashanizadegan, D. M. T. Newsham and N. S. Tavare, Yasuj University, Iran, UMIST, Manchester, UK (on page 60)

17:40 – 18:30 Open Forum with Light Refreshment in Room A

→ Room B: **CHEM. TECH. (Particle Tech.)**

Chair:

9:00 – 10:40

Keynote Address: PROCESS INTENSIFICATION OF PARTICULATE MATERIALS BY PARTICLE COATING, K. Shinohara, Hokkaido University, Japan (onpage 61)

NEW MICROSTRUCTURE DESIGN FOR HARD COMPOSITE MATERIAL BY MECHANICAL COATING OF CERAMIC PARTICLES, S. Kangwantrakool, K. Shinohara, Suranaree University of Technology, Thailand, Hokkaido University, Japan (on page 62)

SOLIDS FLOW AND SEPARATION CHARACTERISTICS ON AN INCLINED FLOW CHUTE WITH DIFFERENT FLOW SURFACES, J. Li, C. Webb, S.S. Pandiella, G.M. Campbell, D.J. Parker & J.P.K Seville, UMIST, UK, University of Birmingham, UK (on page 63)

PROCESS INTENSIFICATION, PROCESS MINIATURIZATION AND INHERENTLY INTENSIVE PROCESSES IN PARTICLE TECHNOLOGY, G. Akay, L. Tong, M. Dogru and R. Adleman, University of Newcastle, Triton Chemical Systems, UK (on page 64)

DETERMINATION OF PHYSICAL PROPERTIES OF SOLID PARTICLES BY USING MINIMUM FLUIDIZATION VELOCITY, M. Levent and S. Yörük, Atatürk University, Turkey, Adviser of Treasury, General Directory of Treasury and Foreign Commerce, Turkey (on page 65)

10:40 – 11:00 Refreshment Break

→ Room B: **ENV. TECH.-II**

Chair:

11:00 – 12:40

Keynote Address: ENHANCED SORPTION OF HEAVY METAL AND ORGANIC CONTAMINANTS USING SURFACTANT-MODIFIED ZEOLITE (SMZ), Pomthong Malakul, Sasitorn Saengchote & David A. Sabatini, Chulalongkorn University, Thailand, University of Oklahoma, USA (on page 66)

APPLICATIONS OF ELECTRO-ELECTRODIALYSIS FOR RECOVERY OF ACIDS FROM PICKLE WASTE IN LEATHER INDUSTRY, E.G. Akgemci, M. Ersöz and T. Atalay, Selcuk University, Turkey (on page 67)

Oxidative Removal of Ethylene by a Multistage Plasma Reactor in the Presence of Sol-Gel TiO_2

K. Saktrakool[1], S. Chavadej[1], P. Rangsunvigit[1], and Lance L. Lobban[2]
[1]The Petroleum and Petrochemical College, Chulalongkorn University, Bangkok 10330, Thailand
[2]School of Chemical Engineering and Materials Science, The University of Oklahoma, Norman, Oklahoma 73019, USA

ABSTRACT

A four-stage plasma and photocatalytic system was set up to study the oxidation of ethylene as a model pollutant. TiO_2 as photocatalyst was prepared by the Sol-Gel method. Both ethylene conversion and CO_2 selectivity were increased with increasing a stage number of the plasma system. The synergistic effect of TiO_2 presented in the plasma reactor is resulted from the activation of TiO_2 by the UV light generated from the plasma. The presence of 1%Pt on sol-gel TiO_2 promoted CO oxidation leading to higher CO_2 selectivity.

INTRODUCTION

Emissions of volatile organic compounds (VOCs) are one of major sources of air pollution (De Nevers, 1995). Air pollutants can enter to the human body mainly by inhalation. Their toxic on human health can cause premature death, respiratory illness, alterations in the lung's defenses, and aggravation of existing cardiovascular disease. Furthermore, these VOCs are important precursors to smog, ozone and acidic precipitation (acid rain) and they can affect both terrestrial and aquatic ecosystems and finally global warming (Papaethimiou *et al.*, 1997). Emissions of VOCs come from many mobile sources and industrial processes including chemical industry and petroleum refineries.

There are various methods for air pollution control, such as liquid absorption, solid adsorption, scrubbing, precipitation, capture device, biodegradation, thermal incineration, and catalytic combustion (Cheng, 1996). Combustion is the most effective way to achieve complete destruction of VOCs as well as gaseous hydrocarbons but energy requirement for combustion is rather high. Non-thermal plasma and photocatalytic processes have been considered as promising alternatives to offer economical operation since they can be operated at ambient conditions. Moreover, main products from these processes are mostly carbon dioxide and water, which are environmental friendly.

For non-thermal plasma, a high voltage is applied across two metal electrodes to produce high-energy electrons that can directly initiate oxidation reaction to decompose organic pollutants. During plasma generation, active species of electrons, radicals, and ions are formed as well as light including UV (Harndumrongsak *et al.*, 2002). Previous work showed that the degradation of ethylene using a combined plasma and photocatalytic reactor, was greatly affected by the residence time (Harndumrongsak *et al.*, 2002).

In this work, a series of reactors with their own plasma generators was developed and tested for the oxidative removal of ethylene. Ethylene was selected as a representative of hydrocarbon pollutants in this study. Moreover, effects of TiO_2, used as a photocatalyst in the plasma reactors on the ethylene removal were investigated.

EXPERIMENT

Materials

Platinum(II)2,4-pentanedionate,$Pt(C_5H_7O_2)_2$ obtained from Alfa Aesar and Tetraethylorthotitanate (TEOT) supplied by Fluga were used as precursors for preparing platinum and titania (TiO_2), respectively. The activity of the photocatalyst prepared by the sol-gel method was compared with Degussa P25, a commercially avaliable titania dioxide obtained from J.J. Degussa Hüls (T) Co. Ltd.

Procedure

A schematic diagram of the experimental set-up in this work is shown in Fig. 1. Experiments were started by introducing reactant gases, 99.99% ethylene, 99.5% oxygen, and 99.95% helium to obtain the feed mixture of 3% ethylene and 15% oxygen with helium balance. The flow rates of these three reactant gases were controlled by mass flow controllers. Before the reactant gases passed through the mass flow controllers, any foreign particles in the feed gases were trapped using 0.7 μm in-line filters. The reactors were made of quartz tubes with 10 mm OD and 8 mm ID. Plasma was generated in each reactor across a pair of stainless steel wire and plate electrodes with a gap distance of 1 cm. The power used to generate plasma was alternative current power, 220V and 50 Hz, which was transmitted to a high voltage side. The output voltage was increased up to 130 times and the signal of the alternative current was a sine form.

After the concentration of the feed mixture was constant, the supply power unit was turned on. After 30 min, the composition of the effluent was analyzed every 30 min until the outlet gas composition was constant. Effects of the stage number of the plasma system on the ethylene removal and product selectivities were investigated by turning off one by one power supply unit of each reactor with the fourth one first.

To investigate the effects of photocatalyst present in the plasma reactors on the ethylene decomposition

and product selectivities, sol-gel TiO_2 or Degussa P25 coated on glass wool is packed in the space between the two electrodes as shown in Fig. 2.

For Degussa P25 coated on glass wool, a sheet of glass wool (3x3 cmxcm) was dipped into a solution of 2% Degussa P25 in distilled water. After that, the glass wool was dried at 100°C for 10 min followed by calcination at 300°C for 3 h. For sol-gel TiO_2 coated on glass wool, 1.5 g of tetraethylorthotitanate (TEOT) was mixed with 20 ml of ethanol and 6 drops of nitric acid to form a gel solution. A sheet of glass wool was dipped into the gel solution. The coated glass wool was dried at 100°C for 10 min, and then calcined at 400°C for 5 h. To prepare 1% Pt/TiO_2, 0.005 g $Pt(C_5H_7O_2)_2$ and 2.83 g of TEOT were dissolved in 38.07 ml of ethanol and 14 drops of nitric acid. The same coating and calculation procedures were carried out as described above.

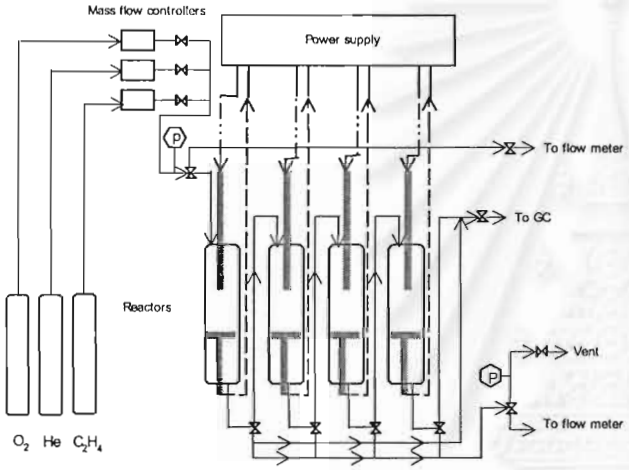

Fig. 1. Schematic diagram of the experimental set-up.

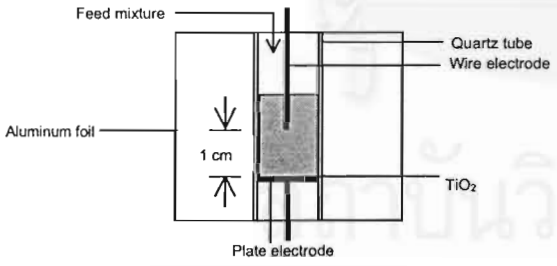

Fig. 2. Configuration of each reactor.

RESULTS AND DISCUSSION

Effects of Frequency

Effect on Ethylene and Oxygen Conversions

Fig. 3 and Fig. 4 show the effects of frequency on C_2H_4 and O_2 conversions, respectively. The conversions of C_2H_4 and O_2 decreased with increasing frequency in the range of 50 to 700 Hz. The explanation is that a higher frequency results in a lower current that corresponds to the reduction of a number of electrons generated (Korada *et al.*, 2003). Consequently, the opportunity of collision between electrons and O_2 molecules decreases. At any fixed frequency, the conversions of C_2H_4 and O_2 increased with the increase in the stage number of reactor since the residence time is increased with increasing the stage number.

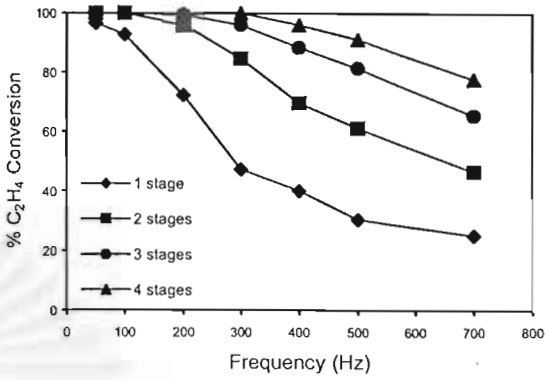

Fig. 3. Effect of frequency on C_2H_4 conversion at a feed flow rate of 160 ml/min, 11,000 V, and a gap distance of 1 cm

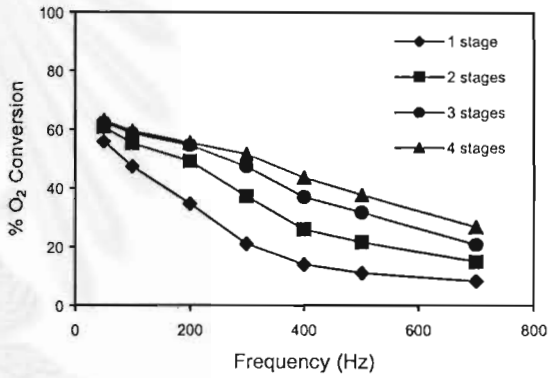

Fig. 4. Effect of frequency on O_2 conversion at a feed flow rate of 160 ml/min, 11,000 V, and a gap distance of 1 cm

Effect on Product Selectivities

The effects of applied frequency on CO and CO_2 selectivities are shown in Fig. 5 and Fig. 6, respectively. When frequency increased, the CO_2 selectivity decreased whereas the CO selectivity increased. As mentioned before, at a lower frequency, there is a larger number of electrons generated from the electrodes leading to more oxygen active species to be produced. Consequently, the reaction between the oxygen active species and CO becomes more effective. For any given frequency, the CO_2 selectivity also increased while the CO selectivity decreased with increasing the stage number of the plasma reactors because the electrons have more chances to break down O_2 to produce the oxygen active species as a result from a longer residence time.

The main effect of frequency on the conversions and selectivities is resulted from the space charge (electrons and ions) characteristics of the discharge,

even though the power is constant. As AC discharge is applied, each electrode performs alternatively as an anode and cathode. The alternating behavior has been proven effectively in eliminating contaminant accumulation on the electrode surface resulting in increasing efficiency as compared to DC discharge (Liu *et al.*, 1996). Based on the results, a frequency of 200 Hz was selected for further studies.

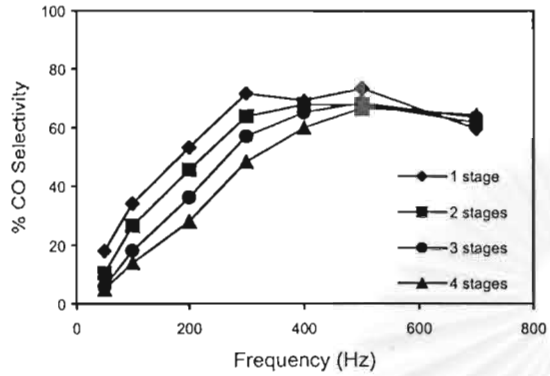

Fig. 5. Effect of frequency on CO selectivity at a feed flow rate of 160 ml/min, 11,000 V, and a gap distance of 1 cm

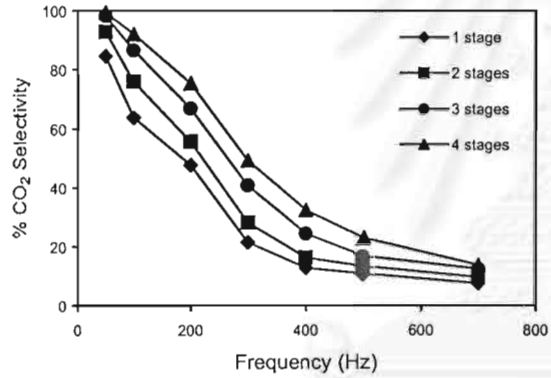

Fig. 6. Effect of frequency on CO_2 selectivity at a feed flow rate of 160 ml/min, 11,000 V, and a gap distance of 1 cm

Effect of Feed Flow Rate

Effects on Ethylene and Oxygen Conversions

Fig. 7 and Fig. 8 illustrate the effects of feed flow rate on C_2H_4 and O_2 conversions, respectively. For either a single or two-stage system, both C_2H_4 and O_2 conversions decreased with increasing the feed flow rate in the studied range because an increase in the feed flow rate corresponds to a decrease in the residence time. For any given feed flow rate, a higher stage number of plasma reactors resulted in higher conversions of both C_2H_4 and O_2. With a decrease in the feed flow rate or an increase in the stage number of plasma reactors in operation, electrons have more possibility to collide with C_2H_4 and O_2 molecules leading to higher conversions of both reactants.

Effect on Product Selectivities

The effects of feed flow rate on CO and CO_2 selectivities are shown in Fig. 9 and Fig. 10, respectively. For any given number of stage, the CO selectivity increased with increasing feed flow rate while the opposite trend was found for the CO_2 selectivity. A higher gas flow rate or a lower of stage number reduces the opportunity of collision between electrons and O_2 molecules. Therefore, the oxidation of CO is reduced resulting in lower CO_2 formation.

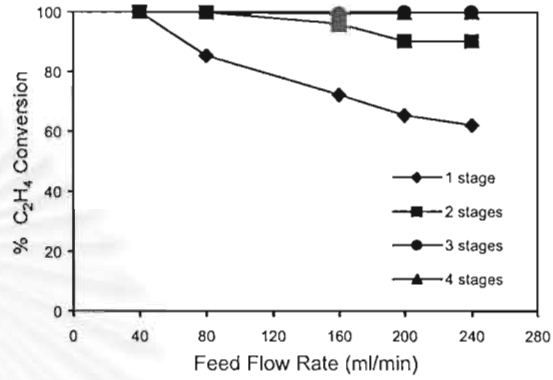

Fig. 7. Effect of feed flow rate on C_2H_4 conversion at 200 Hz, 11,000 V, and a gap distance of 1 cm

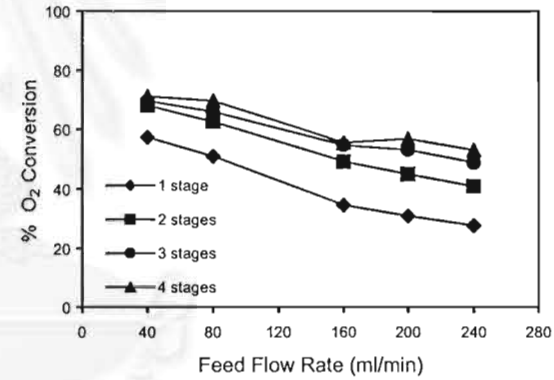

Fig. 8. Effect of feed flow rate on O_2 conversion at 200 Hz, 11,000 V, and a gap distance of 1 cm

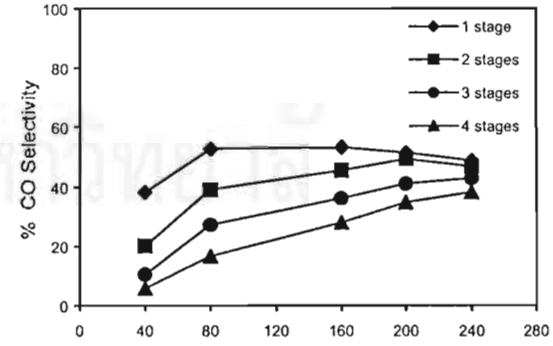

Fig. 9. Effect of feed flow rate on CO selectivity at 200 Hz, 11,000 V, and a gap distance of 1 cm

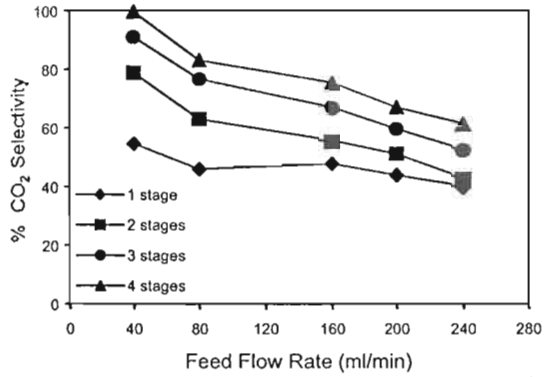

Fig. 10. Effect of feed flow rate on CO_2 selectivity at 200 Hz, 11,000 V, and a gap distance of 1 cm

Effect of Stage Number of Plasma Reactors

Effect on Ethylene and Oxygen Conversions

Fig. 11 shows the effect of stage number of plasma reactor on the C_2H_4 conversion. Under the studied conditions, a complete conversion of C_2H_4 was observed with residence times of 1 and 0.75 sec. However, at the lowest residence time of 0.38 sec, the conversion of C_2H_4 increased with increasing number of stage. As be seen from Fig. 12, for any fixed residence time, an increase in stage number seems not to affect the oxygen conversion.

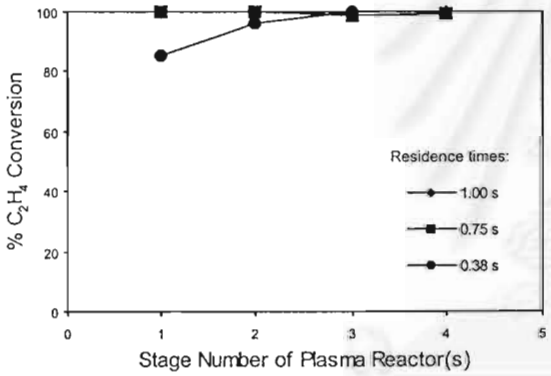

Fig. 11. Effect of stage number on C_2H_4 conversion with different residence times at 200 Hz, 11,000 V, and a gap distance of 1 cm

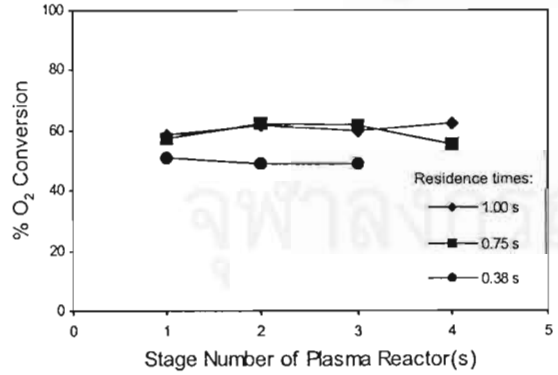

Fig. 12. Effect of stage number on O_2 conversion with different residence times at 200 Hz, 11,000 V, and a gap distance of 1 cm

Effect on Product Selectivities

The effects of stage number on the CO and CO_2 selectivities are shown in Fig. 13 and Fig. 14, respectively. As a stage number of the plasma reactors increased, the CO_2 selectivity increased whereas the CO selectivity decreased. It can be explained that a higher stage number enhance the possibility of the collision between electrons and O_2 molecules; therefore, the oxidation of CO is increased resulting in the higher CO_2 formation.

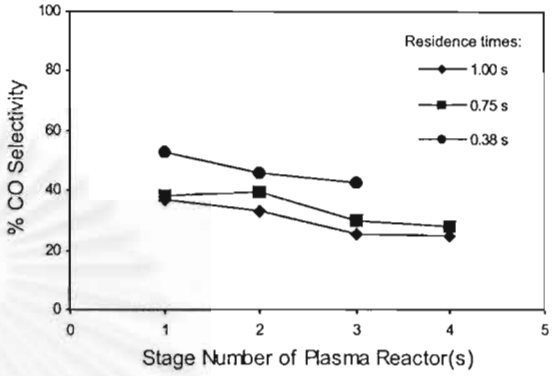

Fig. 13. Effect of stage number on CO selectivity with different residence times at 200 Hz, 11,000 V, and a gap distance of 1 cm

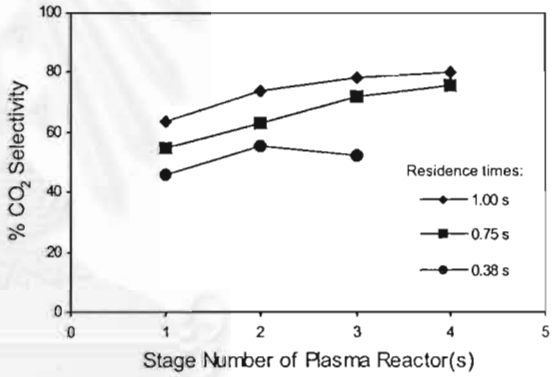

Fig. 14. Effect of stage number on CO_2 selectivity with different residence times at 200 Hz, 11,000 V, and a gap distance of 1 cm

Effect of the Presence of Different Photocatalysts

Effect on Ethylene and Oxygen Conversions

Table 1 shows the effects of the presence of different photocatalysts on conversions and product selectivities. It appeared that the presence of Degussa P25, sol-gel TiO_2 or 1%Pt/sol-gelTiO_2 significantly increased the C_2H_4 conversion by 20% and 10% with 1 and 2 stages in operation, respectively. However, the same effect was not observed when higher than two stages were used. The presence of all studied photocatalysts appeared to increase the O_2 conversion in a following order: 1%Pt/TiO_2 >TiO_2 >Degussa P25 for any given stage number. The results imply that the energy released from the plasma especially in form of UV will excite TiO_2 to create the energy band gap of conductance

band and valance band leading to oxidation and reduction reactions on the TiO_2 surface.

Effect on Product Selectivities

The presence of either sol-gel TiO_2 or the commercial TiO_2 (Degussa P25) increased the CO_2 selectivity by 4-7%, but decreased the CO selectivity by 6%. With 1%Pt loaded on sol-gel TiO_2, the CO_2 selectivity increased significantly about 10-17%. Since Pt on TiO_2 attributes to the acceleration of superoxide radical anion, $O_2^{\bullet-}$, formation and consequently decreases the recombination process leading to enhance the photocatalytic activity (Blazkova *et al.*, 1998).

Table 1. Comparative results of the plasma system with and without photocatalyst (at 160 ml/min flow rate, 9000 V, 200 Hz, 1 cm gap distance and 0.008 g photocatalyst)

Reactor	% Conversion		% Selectivity	
	C_2H_4	O_2	CO	CO_2
No catalyst				
1st	47	22	70	29
2nd	80	37	61	35
3rd	95	47	52	46
4th	99	52	43	56
Commercial TiO_2 (Degussa P25)				
1st	67	30	58	36
2nd	90	43	56	42
3rd	98	50	48	51
4th	99	53	41	60
TiO_2 (sol-gel)				
1st	68	33	57	38
2nd	90	44	55	43
3rd	99	50	48	51
4th	99	54	41	60
1% Pt/TiO_2 (sol-gel)				
1st	68	35	56	46
2nd	90	46	55	46
3rd	98	53	46	56
4th	99	57	35	70

CONCLUSIONS

From the experimental results of the sole plasma system and the plasma system combined with photocatalyst, the ethylene was almost completely removed by the corona discharge especially with 4 stages. The ethylene removal efficiency decreased with increasing frequency since a higher frequency results in lowering current that corresponds to the reduction of the number of electrons generated. A higher feed flow rate decreased the C_2H_4 and O_2 conversions and CO_2 selectivity as a result from decreasing residence time. An increase in the stage number increased remarkably both C_2H_4 conversion and CO_2 selectivity. The presence of photocatalysts, commercial TiO_2 (Degussa P25) and TiO_2 prepared by sol-gel method, enhanced both C_2H_4 and O_2 conversions as well as CO_2 selectivity because the UV light liberated from plasma generation activates TiO_2 to promote complete oxidation reaction. As expected, the presence of 1%Pt on TiO_2 increased the CO_2 selectivity compared to Degussa P25 and TiO_2 as a result from Pt producing superoxide radical anion, $O_2^{\bullet-}$, and decreasing the recombination process.

ACKNOWLEDGEMENTS

Ratchadapiseksompoch Fund provided by Chulalongkorn University for partial support of this project and National Petrochemical (Public) Co. Ltd. for donating ethylene are acknowledged.

REFERENCES

1. Blazkova, A., Csolleova, I., and Brezova, V. (1998). Effect of light sources on the phenol degradation using Pt/TiO_2 photocatalysts immobilized on glass fibers. *Journal of Photochemistry and Photobiology A: Chemistry*, 113, 251-256.
2. Cheng, Y. (1996). *Kinetic and Mechanistic Studies of Volatile Organic Compound Oxidation Catalysis Using Thin Film Model Pt Catalysts.* A Research Proposal Submitted in partial Fulfillment of The Preliminary Examination Requirements, The University of Michigan.
3. De Nevers N. (1995*). Air Pollution Control Engineering.* International Editions. New York: McGRAW-HILL.
4. Harndumrongsak, B., Lobban, L.L., Rangsunvigit, P., and Kitiyanan, B. (2002). Oxidation of Ethylene in plasma environment. *Proceeding of the 9th APCChE Congress,* Christchurch, New Zealand, 29 September – 3 October 2002.
5. Supat, K., Chavadej, S., Lobban, L.L., and Mallinson, R.G. (2003). Synthesis gas production from partial oxidation of methane with air in ac electric gas discharge, *Energy&Fuels* (In Press).
6. Liu, C., A. Marafee, B. Hill, G. Xu, R. G. Mallinson, and L. Lobban, "Oxidative Coupling of Methane with ac and dc Corona Discharge," *Ind. Eng. Chem. Res.*, 35, 3295 (1996).
7. Papaethimiou, P., Ioanides, T., and Verykios, X.E. (1997). Combustion of non-halogenated volatile organic compounds over group VIII metal catalysts. *Applied Catalysis B: Environmental*, 13, 175-184.